MASTERARBEIT | MASTER'S THESIS

Titel | Title

Biochemical and pharmacological investigations to determine whether GABA is a substrate at the vesicular monoamine transporter VMAT2

verfasst von | submitted by

Fabian Limani BSc

angestrebter akademischer Grad | in partial fulfilment of the requirements for the degree of

Master of Science (MSc)

Wien | Vienna, 2024

Studienkennzahl lt. Studienblatt | Degree programme code as it appears on the student record sheet:	UA 066 863
Studienrichtung lt. Studienblatt | Degree programme as it appears on the student record sheet:	Masterstudium Biologische Chemie
Betreut von | Supervisor:	ao. Univ.-Prof. Mag. Dr. Peter Fuchs Privatdoz.

Abstract

Midbrain dopamine (DA) neurons, which have important functions in reward and locomotion, are composed of different subpopulations. Some of them are not only expressing transporters needed to sequester and release DA (the plasmalemmal dopamine transporter (DAT)) and the vesicular monoamine transporter (VMAT2)), but also for example the vesicular glutamate transporter (VGLUT2) so they can co-release glutamate, the main excitatory neurotransmitter. In contrast, co-release of γ-aminobutyric acid (GABA), the major inhibitory neurotransmitter, does not seem to depend on the classical machinery thought to be necessary for GABA release. In contrast, it has been proposed that GABA is taken up into DA neurons via the plasmalemmal GABA transporter (GAT1) and then packaged into synaptic vesicles by VMAT2. So far, GABA co-release from DA neurons has only been indirectly shown by measurement of inhibitory postsynaptic currents (iPSCs) at $GABA_A$ receptors, which could also be induced by other neurotransmitters/ligands.

My goal was to find out, whether GABA is a substrate at VMAT2 and if there is an interaction between GAT1 and VMAT2. In order to address these questions, I performed radiotracer flux measurements in synaptic vesicles isolated from different species and started to perform co-immunoprecipitation and immunoblotting experiments.

While the co-immunoprecipitation experiments have not yielded unequivocal results during the time of my thesis work, my uptake assays indicate that GABA reduced the uptake of [^{3}H]serotonin, an endogenous VMAT2 substrate, at millimolar concentrations, suggesting that GABA could indeed be a low-affinity substrate at VMAT2.

Zusammenfassung

Dopamin (DA)-produzierende Neurone im ventralen Mittelhirn spielen eine wichtige Rolle bei Belohnung und Bewegung und bestehen aus verschiedenen zellulären Subpopulationen. Einige der Neurone exprimieren nicht nur Transporter zur Speicherung und Ausschüttung von DA (nämlich den plasmalemmalen Dopamintransporter (DAT) und den vesikulären Monoamintransporter (VMAT2)), sondern etwa auch den vesikulären Glutamattransporter (VGLUT2). Die VGLUT2-exprimierenden DA Neurone können dadurch neben DA auch Glutamat, den wichtigsten exzitatorischen Neurotransmitter, ausschütten. Im Gegensatz dazu scheint die zusätzliche Freisetzung von γ-Aminobuttersäure (GABA), dem wichtigsten inhibitorischen Neurotransmitter, nicht von der kanonischen Maschinerie für Synthese und Speicherung von GABA abhängig zu sein. Es wurde jedoch postuliert, dass DA Neurone GABA durch den plasmalemmalen GABA-Transporter (GAT1) in die Zellen aufnehmen und dann GABA mittels VMAT2 in die synaptischen Vesikel aufnehmen. Bis jetzt wurde die Ausschüttung von GABA aus DA-Neuronen nur indirekt durch Messung von inhibitorischen postsynaptischen Strömen (iPSCs) an $GABA_A$ Rezeptoren gezeigt, die aber theoretisch auch durch andere Neurotransmitter/Liganden induziert werden könnten.

Das Ziel meiner Masterarbeit war es herauszufinden, ob GABA ein Substrat für VMAT2 ist und ob es eine Interaktion zwischen GAT1 and VMAT2 gibt. Um das zu testen, habe ich Messungen mit radioaktiv markierten Transmittern in isolierten synaptischen Vesikeln aus Nagetieren, nichtmenschlichen Primaten und Menschen gemacht, sowie Co-Immunopräzipitationen und Immunoblots durchgeführt.

Während ich in den Co-Immunopräzipitation-Experimenten noch keine eindeutigen Ergebnisse erhalten habe, zeigen meine Uptake-Assays, dass GABA die Aufnahme von [^{3}H]Serotonin, einem endogenen VMAT2-Substrat, in millimolaren Konzentrationen vermindern konnte. Dies deutet darauf hin, dass GABA für VMAT2 ein Substrat mit niedriger Affinität sein könnte.

Acknowledgements

First, I would like to thank my supervisor Dr. Thomas Steinkellner from the Institute of Pharmacology at the Medical University of Vienna, where I performed all my experiments, for making this thesis possible in the first place. I felt very welcome in the laboratory from the start and could at any time discuss my plans, concerns, experiments etc. with Thomas, who introduced me to all the pharmacological methods. I was not only given the opportunity to gain general as well as field-specific scientific knowledge, but also to practice and refine my presentation skills through our weekly lab meetings, a journal club and by presenting my results during a 'thesis seminar' for PhD students. The highlight of course was the FENS forum 2024, Europe's biggest congress for neuroscientists, where I could present a poster. Although in the beginning it was a bit of a challenge for me, I'm also grateful for working in an international group of scientists coming from India, Egypt, Finland, USA, Spain, France and Canada, showing me also sometimes different approaches to a topic and giving me insights into other cultures.

Here, I also want to express my gratitude towards all my colleagues from the Steinkellner Lab and our office, who always helped me with advice and showed me around the laboratory, as well as creating a good working atmosphere. I want to especially highlight Michael and Iina, two fellow Master students, who initially introduced me to the lab, the cell culture work there and uptake assays and the PhD student Siva, from whom I gained a lot of information and insight into this scientific field but also in a more general sense, who I had a lot of good talks with and also shared some projects and experiments.

In the end, I want to also thank my mother and stepfather for always supporting me as well as helping me to stay focussed, motivated and to ask others and myself interesting questions to learn more about science and biochemistry.

List of abbreviations

5-HT	5-Hydroxytryptamine (serotonin)
AMPA	α-Amino-3-hydroxy-5-methyl-4-isoxazole proprionic acid receptor
CNS	Central nervous system
DA	Dopamine
DTBZ	Dihydrotetrabenazine
EAATs	Excitatory amino acid transporters
FFN206	Fluorescent false neurotransmitter 206
FFPE	Formalin-fixed paraffin-embedded
GABA	γ-Aminobutyric acid
GAD	Glutamic acid decarboxylase
GAT1	GABA transporter 1
IP	Immunoprecipitation (buffer)
KP	Potassium phosphate (buffer)
NFDM	Non-fat dry milk
NMDA	N-Methyl-D-aspartate receptor
PD	Parkinson's disease
PEI	Poly(ethyleneimine)
RFU	Relative fluorescence units
SDS-PAGE	Sodium dodecyl sulphate polyacrylamide gel electrophoresis
SNc	Substantia nigra *pars compacta*
TBST	Tris-buffered saline with 0.1% tween
TBZ	Tetrabenazine
VGAT	Vesicular GABA transporter
VGLUT1-3	Vesicular glutamate transporter 1-3
VMAT2	Vesicular monoamine transporter 2
VTA	Ventral tegmental area

Table of contents

1 Introduction

1.1 Neurotransmitter packaging and release

Neurotransmitters generally act as chemical messengers between neurons to pass on information. In order to be released from the pre-synaptic neuron upon receiving an electrical signal and thus depolarisation or hyperpolarisation of the membrane, neurotransmitters must first be loaded into synaptic vesicles, before fusing with the presynaptic membrane and release of the neurotransmitter molecules into the synaptic cleft (Fon and Edwards 2001).

First of all, the neurotransmitters must be present in the cytosol, either via direct biosynthesis from precursor molecules or by importing a transmitter from outside the cell. In order for the transmitters to cross lipid membranes, specialised transmembrane transporters are required. For example, vesicular uptake of transmitters requires vesicular transmitter transporters such as the vesicular glutamate transporter (VGLUT1-3) for glutamate, the vesicular GABA transporter (VGAT) for GABA and glycine or the vesicular monoamine transporter (VMAT2) for monoamines (dopamine, noradrenaline, adrenaline, serotonin, histamine) (Lin et al. 2015; Pidathala et al. 2023). For the vesicular transmitter transporters, the main driving force is the electrochemical H^+ gradient that is established by the vacuolar proton ATPase (vATPase). The H^+ gradient consists of two parts: the pH and an electrical gradient; different transmitters depend differently on the two parts (Johnson et al. 1981; Cidon and Sihra 1989; Edwards 2007). For instance, for the uptake of the positively charged monoamine DA, the pH gradient is more important than the electrical gradient while for the negatively charged amino acid glutamate, the electrical gradient is more important (Maycox et al. 1988). This is because the cationic DA is exchanged for two lumenal H^+, which means that in total one positive charge is exchanged for two H^+ and results in a greater pH gradient dependence (Knoth et al. 1981). For anionic glutamate the stoichiometry is not known, but in total there always is one more charge exchanged than H^+, which results in greater dependence on the electrical gradient (Edwards 2007).

The uptake of extracellular neurotransmitters is achieved by transporters from the SLC6 family of neurotransmitter:sodium symporters, as well as from the SLC1 family (Lin et al. 2015). These rely on the electrochemical Na^+ gradient to transport transmitters against their concentration gradients, some transporters of the SLC6 family are additionally dependent on co-transport of Cl^- and K^+. The first transporter of the SLC6 family to have been molecularly characterised was the GABA transporter 1 (GAT1, SLC6A1), which is the main (plasmalemmal) GABA transporter in the brain (Chen et al. 2004).

1.2 Glutamate as a neurotransmitter

Glutamate is known to affect the central nervous system (CNS) for a long time, but was acknowledged as an (excitatory) neurotransmitter only in 1984 (Fonnum 1984). For intracellular *de novo* biosynthesis, first glucose is metabolized to pyruvic acid during glycolysis and pyruvate then enters the tricarboxylic acid (TCA) cycle during which α-ketoglutarate is generated, and finally transaminated to yield glutamate (Hertz et al. 1999). As a consequence, glutamate was found to be present in all (CNS) cell types, also because of its role as building block for proteins (Watkins and Jane 2006). For the synaptic release of glutamate, the vesicular glutamate transporters 1, 2 and 3 (VGLUT1-3) are needed (Takamori 2006) to store glutamate within synaptic vesicles. Glutamate is then released through vesicular exocytosis and acts via two major types of glutamate receptors: ionotropic receptors (those are ion channels that transport cations like Na^+ and Ca^{2+}, i.e. N-Methyl-D-aspartate (NMDA), α-Amino-3-hydroxy-5-methyl-4-isoxazole proprionic acid (AMPA) and kainate (KA) receptors) and metabotropic receptors (called mGluR 1-8, those are G protein-coupled receptors with for instance effects on second messenger systems) (Niciu et al. 2012).

High levels of extracellular glutamate lead to cell damage or even neuron cell death because of sustained depolarisation via ionotropic glutamate receptors (Li and Stys 2000). This can trigger influx of Na^+, Cl^- and water, leading to swelling as well as sustained influx of Ca^{2+} starting several destructive cascades (Choi 1992). Therefore, after release it has to be removed in the course of milliseconds: glutamate is primarily removed from the synaptic cleft by transporting it into the cytosol of glial cells via excitatory amino acid transporters (EAATs), where it is then converted to glutamine and transported out of glial cells. Glutamine can then be taken up again by neurons and be converted to glutamate by glutaminase (Niciu et al. 2012).

1.3 GABA as a neurotransmitter

γ-aminobutyric acid (GABA) is the major inhibitory neurotransmitter and is synthesized from glutamate by either of two isoforms of glutamic acid decarboxylase GAD65 and GAD67 (also known as GAD2 and GAD1, respectively). In midbrain dopamine (DA) neurons it was shown that there may to be another non-canonical pathway for GABA biosynthesis mediated by aldehyde dehydrogenase 1a1 (ALDH1a1) (Kim et al. 2015), but the role of this enzyme in GABA synthesis remains controversial (Melani and Tritsch 2022). Extracellular GABA can be taken up into cells by plasmalemmal GABA transporters like the GABA transporter 1 (GAT1). In order to release GABA synaptically, the vesicular GABA transporter (VGAT) is needed to package GABA into synaptic vesicles. Synaptic GABA exerts its action via activation of mostly $GABA_A$ and $GABA_B$ receptors. $GABA_A$ receptors are ionotropic receptors that mediate Cl^- conductance, while $GABA_B$ receptors are metabotropic receptors (Zhang et al. 2021).

1.4 Midbrain dopamine system

The midbrain dopamine (DA) system mainly consists of the ventral tegmental area (VTA) and the substantia nigra *pars compacta* (SNc), which are both heavily projecting to the striatum (Fuxe et al. 2010). Despite the VTA and the SNc being relatively small regions (Nelson et al. 1996; Björklund and Dunnett 2007), the DA system is of high interest since there are many neuropsychiatric diseases like Parkinson's disease (PD), schizophrenia and substance use disorders associated with dysfunction of the DA system (Bissonette and Roesch 2016; Limani et al. 2024).

Initially, it was thought that DA neurons are a homogenous cell population with all neurons being relatively similar because of synthesising and releasing the neurotransmitter DA. For a long time it was assumed that one neuron only releases one neurotransmitter, which is referred to as 'Dale's principle' (Strata and Harvey 1999; Tritsch et al. 2016). Nevertheless, over the last few decades it was recognised that the DA system is much more complex and heterogenous because of different DA neuron subpopulations, co-releasing other neurotransmitters, too (Tritsch et al. 2016). For instance, it is already well established that subpopulations of DA neurons are expressing the vesicular glutamate transporter 2 (VGLUT2) (Trudeau et al. 2014), which is both necessary and sufficient for storage and release of glutamate, since the major excitatory neurotransmitter is already present in all neurons in millimolar concentrations (Featherstone 2010; Limani et al. 2024). It seems that expression of VGLUT2 facilitates packaging of DA into synaptic vesicles ('vesicular synergy') (Hnasko et al. 2010) and is preventing degeneration of DA neurons (Steinkellner et al. 2018; 2022). While it has been shown that there are also DA neurons that can co-release γ-aminobutyric acid (GABA) (Tritsch et al. 2012), the mode of action is less well defined since the classical enzymes for synthesis of GABA, glutamic acid decarboxylase 1 and 2 (GAD1/2, also GAD65/67), and the vesicular GABA transporter (VGAT) are only weakly expressed in DA neurons (Melani and Tritsch 2022). The functions of GABA co-release are not well known, but may include spatially and temporally more precise signals and regulation of synaptic plasticity (Tritsch et al. 2016).

1.5 GABA was never directly shown to be a VMAT2 substrate

As mentioned above, co-release of glutamate, the main excitatory neurotransmitter, from DA neurons is well established (Eskenazi et al. 2021), while not so much is known about co-release of GABA, which is the major inhibitory neurotransmitter in the brain (Bowery and Smart 2006). One reason for why GABA release from DA neurons is controversial is that DA neurons do not possess the canonical machinery associated with GABA synthesis and release, namely GAD1 and GAD2 and the vesicular GABA transporter VGAT to load it into synaptic vesicles (Tritsch et al. 2012; 2014).

In the experiments of Tritsch et al., they measured optogenetically evoked inhibitory postsynaptic currents (oIPSCs) at $GABA_A$ receptors, which they did using whole-cell voltage-clamp recordings in striatal neurons (Tritsch et al. 2012; 2014; Melani and Tritsch 2022). After knocking out VGAT in GABAergic neurons, oIPSCs could mostly be restored by introducing ectopic VMAT2 (Tritsch et al. 2012). In contrast, knockout of VGAT from DA neurons did not influence oIPSCs (Tritsch et al. 2012), presumably because VGAT is not playing a major role in vesicular GABA transport within DA neurons. In another set of experiments, Tritsch and colleagues performed experiments where they could abolish oIPSCs by knocking out GAT1 in DA neurons and they were able to restore it by introducing GAD67, which is a GABA synthetic enzyme (Melani and Tritsch 2022). Taken together, these results indicate that GABA is released from DA neurons and that the release is dependent on VMAT2. It has to be mentioned though that the measured oIPSCs could theoretically be caused by other ligands/$GABA_A$ receptor agonists besides GABA, i.e. glycine or taurine **(Figure 1)** (Jonas et al. 1998). This is because by measuring oIPSCs, one only knows that the $GABA_A$ receptor was activated, but not which molecule led to its activation in the first place.

It is also important to bear in mind that GABA looks structurally quite different from the typical VMAT2 substrates (**Figure 1**) which are positively charged monoamines under physiological conditions, while GABA is an amino acid and has no net charge (**Figure 2**). As can also be seen seen in **Figure 2**, the ratio of GABA ionic species is influenced by the pH – at pH 3.5 about half of the species is present in its anionic form and at pH 10.5 approximately half of the GABA population is in its cationic form (Krishek et al. 1996).

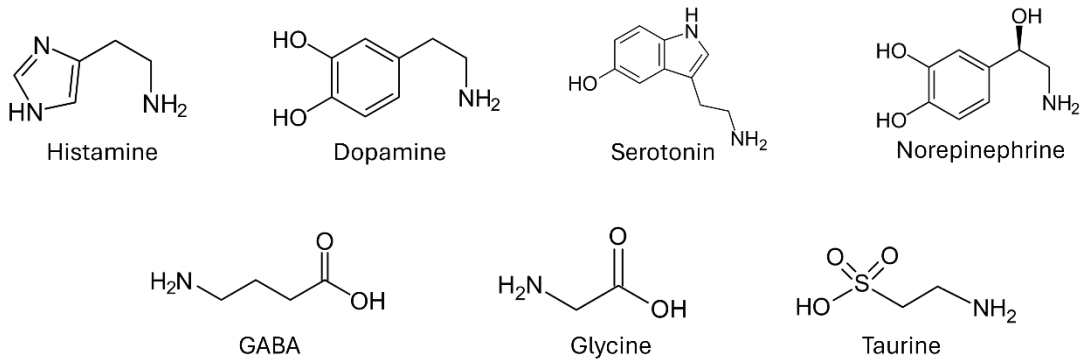

Figure 1: Structures of typical VMAT2 substrates and possible $GABA_A$ receptor substrates. *Typical VMAT2 substrates (histamine, dopamine, serotonin and norepinephrine) are monoamines with a positive charge under physiological conditions, while GABA is an amino acid with no net charge. The amino acids glycine and taurine are possible substrates at $GABA_A$ receptors like GABA. Created using ACD/ChemSketch.*

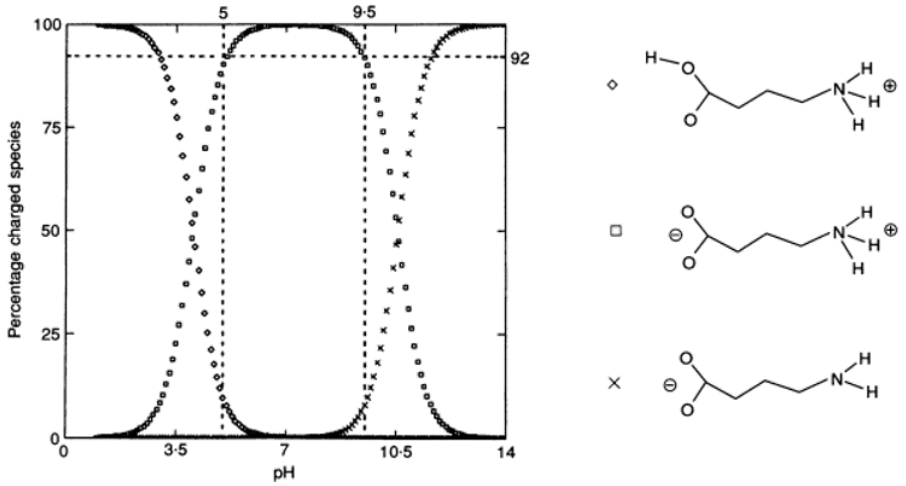

Figure 2: Net charge of GABA is pH-dependent. *At physiological conditions (ca. pH 7.2), GABA is only present in its zwitterionic form with no net charge. Around pH 3.5, half of the molecules is positively charged and around pH 10.5, half of the molecules is negatively charged. Figure is taken from (Krishek et al. 1996)*

2 Materials and methods

2.1 Materials

Table 1: Used reagents and sources.

Reagent/Resource	Source	Details
Antibodies		
Mouse anti-GFP antibody	Santa Cruz	#sc-9996
Rabbit anti-GFP antibody	Invitrogen	#A-11122
Rabbit anti-GAT1 polyclonal antibody	Synaptic Systems	#274 102
Rabbit anti-VMAT2 polyclonal antibody	Synaptic Systems	#138 313
Goat anti-Mouse	LI-COR	IRDye 680RD, #926-68070
Goat anti-Rabbit	LI-COR	IRDye 680RD, #926-68071
Radiolabelled substrates		
[^{3}H]DTBZ	American Radiolabelled Chemicals	(±)-α-[2-^{3}H]-Dihydrotetrabenazine, 20 Ci/mmol
[^{3}H]GABA	Revvity	Aminobutyric Acid (GABA) γ-[2,3-^{3}H(N)]-, Specific Activity: 25-40 Ci (925 GBq-1.48 TBq)/mmol, 250 µCi (9.25 MBq)
[^{3}H]GABA	Revvity	Aminobutyric acid, γ-[2,3-^{3}H(N)]-(GABA), 29.1 Ci/mmol, 1 mCi/mL
[^{3}H]5-HT	Revvity	5-[1,2-^{3}H(N)]-hydroxytryptamine creatinine sulfate, 1 mCi/mL, 32.8 Ci/mmol
General		
FFN206	Tocris	False fluorescent neurotransmitter dihydrochloride
Tetrabenazine	Selleckchem	
Reserpine	Sigma-Aldrich	
Scintillation cocktail	Roth	ROTISZINT®Routine
GF/B filters	GE Healthcare/Whatman	Glass microfiber filters
ATP-Mg	Sigma-Aldrich	Adenosine 5'-triphosphate magnesium salt
GABA	Sigma-Aldrich	
Protein ladder	Thermo Scientific	PageRuler
Nitrocellulose blotting membrane	Cytiva	Amersham Protran Premium 0.45 µm NC
Protein G beads	Cytiva	GammaBind Plus Sepharose, #17088601
96/24-well plate	Sarstedt	Standard F
Cell culture medium	Capricorn Scientific	DMEM, high glucose (4.5 g/L) with L-glutamine

Table 2: Used devices and brands.

Device	**Brand**	**Model**
Table centrifuge	Eppendorf	5427 R
Ultracentrifuge	Beckman	L-70 with TYPE65 rotor
Fluorescence scanner	LI-COR	ODYSSEY CLx
Epifluorescent microscope	Nikon	Eclipse TS100
Liquid scintillation counter	PerkinElmer	Tri-Carb 2800TR
Liquid scintillation counter	Revvity	Tri-Carb 4910 TR
Plate reader	PerkinElmer	1420 VICTOR3 V multilabel counter

2.2 Animals

In this study adult male and female C57BL/6J mice (from a Vglut2-ires-cre background) and adult female Sprague-Dawley rats were used. For details regarding housing and protocols see (Limani et al. 2024). All animal protocols have been approved by the pertinent authorities.

Nonhuman primate (M. fascicularis) striata have been obtained from Dr. Christian Pifl (Center for Brain Research, Medical University of Vienna) through a collaboration with Dr. Jose Obeso (CEU San Pablo University Madrid).

2.3 Human tissue

De-identified formalin-fixed paraffin-embedded sections (FFPE) from the midbrain as well as frozen striata were obtained from the neuro biobank of the Division of Neuropathology and Neurochemistry/Department of Neurology at the Medical University of Vienna and some of the frozen striata were also obtained from Dr. Christian Pifl (Center for Brain Research, Medical University of Vienna); these cases have also been used and published by Dr. Pifl (Pifl et al. 2023).

2.4 Cell culture

HEK293 cells were purchased from ATCC (CRL-1573, ATCC, Manassas, VA, USA; RRID: CVCL_0045). A polyclonal HEK293-VMAT2 cell line was used and generated through blasticidin S (Thermo Fisher Scientific; 10 µg/mL) by transfecting HEK293 cells with human VMAT2-eGFP in pcDNA6.2 using jetPRIME (Polyplus) by Dr. Thomas Steinkellner. N2a cells were a gift from Dr. Erik Keimpema (Center for Brain Research, Medical University of Vienna). N2a cells were transiently transfected with a rat GAT1-eYFP or human VMAT2-YFP plasmid in pcDNA using jetPRIME.

Cells were maintained in Dulbecco's modified eagle medium (DMEM; Capricorn Scientific) containing 10% fetal bovine serum (Sigma-Aldrich), penicillin (100 IU/mL, Sigma-Aldrich), streptomycin (100 µg/mL, Sigma-Aldrich) and for the HEK293-VMAT2 cell line also blasticidin S (6 µg/mL). Cells were maintained in a humidified 5% CO_2 atmosphere at 37°C.

2.5 Radiotracer uptake and binding assays

Radiotracer uptake and binding assays are used to study drug-transporter interactions (Ilic et al. 2020), in this case they are performed in synaptic vesicles. For uptake assays, isolated synaptic vesicles are incubated in a buffer containing radiolabelled substrates for the vesicular transporter VMAT2. The suspension is then filtered after stopping the uptake and washing away all excess radiolabelled molecules outside the synaptic vesicles, using a special filtration chamber (**Figure 3**). These filters are then placed in vials containing a scintillation cocktail by putting them into a liquid scintillation counter, the amount of radioactivity inside the synaptic vesicles can be measured (a schematic can be seen in **Figure 4**). Also, other non-labelled substances can be added during an uptake assays to determine whether uptake of the measured radiolabelled substrate is affected by doing so and to what extent. The principle of binding assays is similar, but now the synaptic vesicles are incubated with a radiolabelled inhibitor of VMAT2 and the amount of inhibitor bound to the transporter is measured. In this case, [^{3}H]dihydrotretrabenazine (DTBZ) is used, which is an analogue of the high affinity VMAT2 inhibitor tetrabenazine (TBZ).

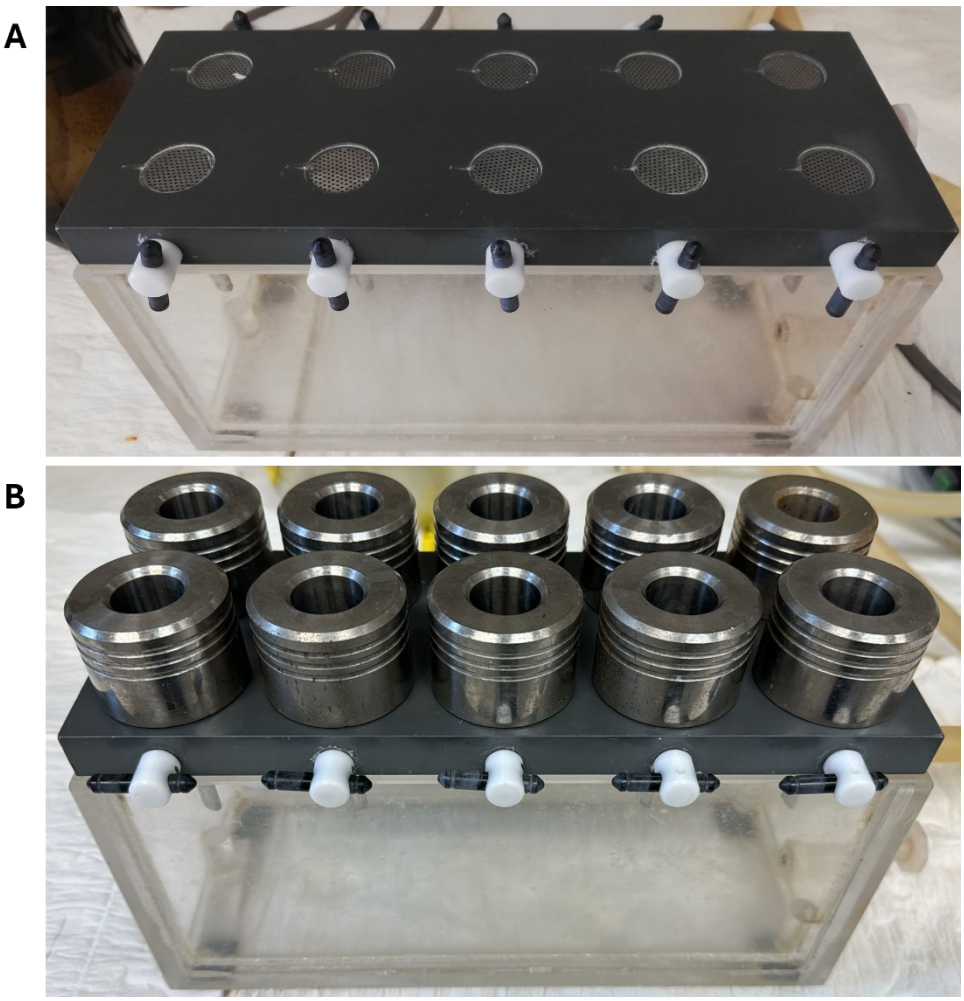

Figure 3: Filtration chamber for uptake and binding assays with synaptic vesicles. *On the side of the grey top-piece, valves for opening and closing the individual channels can be seen. On the metal grids seen in* ***(A)****, filters of the same shape and size are placed and then on top there are metal cylinders* ***(B)*** *to fill with the suspension to be filtrated. The filtration is driven by a vacuum inside the chamber.*

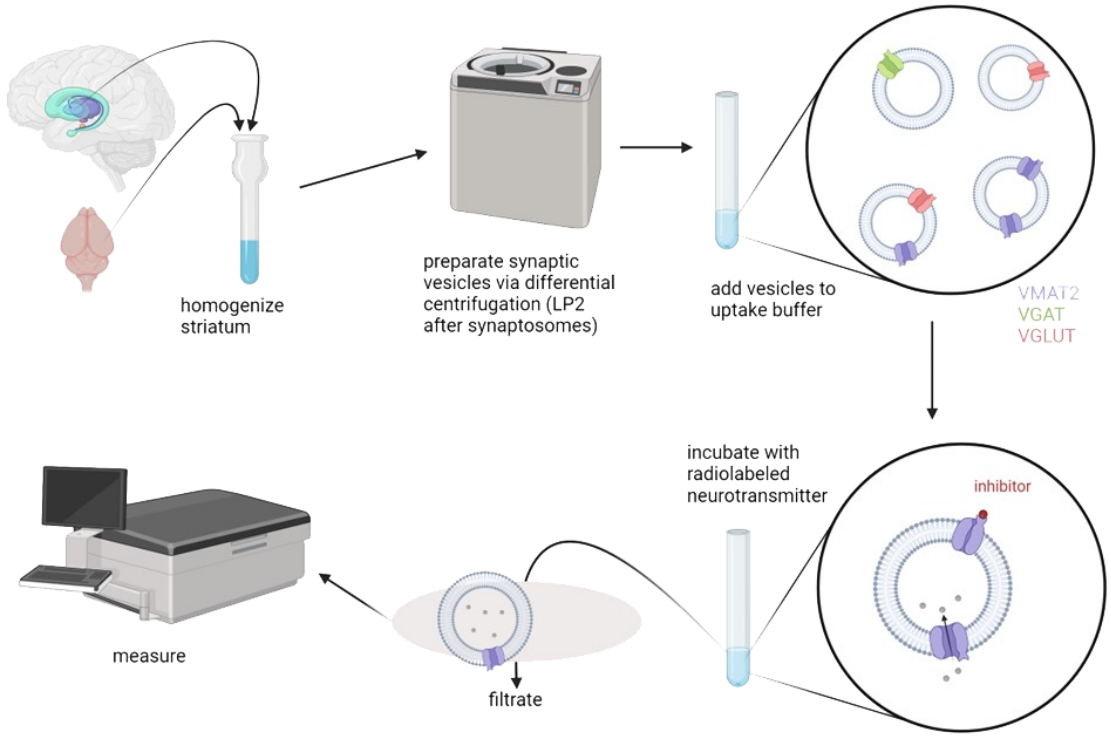

Figure 4: Schematic for the procedure of an uptake assay with synaptic vesicles. *After homogenizing tissue from the region of interest, synaptic vesicles are prepared via differential centrifugation, meaning that with each centrifugation step the time and/or relative force is increased and after the last step in an ultracentrifuge, the vesicles are resuspended in buffer. This suspension with mixed vesicle populations, containing different (combinations of) transporters, is then incubated in uptake buffer containing radiolabelled substrate (and non-labelled testing substances). After stopping the incubation, the suspension is filtrated and washed. The amount of radioactivity inside the vesicles is measured with a liquid scintillation counter. The figure was created using BioRender.*

2.5.1 Synaptic vesicle preparation

With slight modifications, for the synaptic vesicle preparation I followed Dr. Christian Pifl's protocol (Pifl et al. 2014). First, mice were deeply anaesthetised with pentobarbital (100 mg/kg i.p.; Exagon® 500 mg/mL, Richter Pharma) before decapitation. Rats were euthanised by CO_2 asphyxiation and then decapitated. Mouse and rat brains were quickly removed and striatum and cerebellum (only mice) were homogenised in ice-cold 0.32 M sucrose containing 0.25 mM Tris-HCl (pH = 7.4), using a glass Teflon Potter-type homogeniser (20 strokes). Monkey and human striatum tissue chunks were already dissected by Drs. Jose Obeso and Christian Pifl and stored at -80°C. The homogenates were then centrifuged for 15 min at 1,000 x g at 4°C and the supernatant was again centrifuged for 30 min at 20,000 x g at 4°C, resulting in a 'P2' pellet. While ultracentrifuging the supernatant 'SN2' for 30 min at 100.000 x g at 4°C, the P2 pellets were hypoosmotically shocked by resuspension in ice-cold ddH_2O and 10 more strokes in the

glass Teflon Potter-type homogeniser. The aqueous P2 suspensions were centrifuged for 15 min at 21,000 x g at 4°C and osmolarity of the supernatant was restored by adding 1.3 M potassium phosphate (KP) buffer (pH = 7.4) in 1/10 of the volume (final 0.13 M). The SN2 pellets from the ultracentrifuge were then resuspended in the hypoosmotically shocked P2 suspensions and centrifuged for 45 min at 100,000 x g at 4°C. The resulting 'LP2' pellets were resuspended in 0.13 M KP buffer and kept on ice or stored at -80°C until the start of the experiment. The 'LS2' supernatants were also kept at -80°C.

2.5.2 Radioligand uptake

Uptake in synaptic vesicles was performed in 0.13 M KP buffer containing 2 mM ATP-Mg, 2 mM KCl and either [^{3}H]5-HT (100 nM) or [^{3}H]GABA (50 nM from a 75.3 Ci/mmol stock or 344 nM from a 29.1 Ci/mmol stock). The 29.1Ci/mmol [^{3}H]GABA stock (344 nM solution) had a lower specific activity and therefore higher concentration, meaning that in the same volume there are more GABA molecules labelled with the radioisotope, leading to stronger signals. Using concentrations of [^{3}H]GABA near the apparent K_M at VGAT and VMAT2 would be best for clear results, so this higher concentrated stock could be important because of the low affinity of GABA at VGAT and VMAT2. Additionally, unlabelled GABA was added at a putative saturating concentration of 30 mM to block [^{3}H]GABA uptake via VGAT (Takamori et al. 2000). After adding synaptic vesicles to the solution, the uptake was started by putting the tubes into a water bath at 30°C. Incubation time was either 5 min (5-HT), 10 min (344 nM GABA) or 15 min (50 nM GABA) and the uptake was stopped by addition of ice-cold KP buffer to the tubes, filtration of the suspension through poly(ethyleneimine)-coated (1% w/v) GF/B glass fiber filters (Whatman) and two additional washes with 2 mL KP buffer. The filters were then transferred to scintillation vials, vortexed and measured in a liquid scintillation counter (PerkinElmer/Revvity). Each vesicle uptake was performed in duplicate determinations. Additionally, a filter blank (treated like all other tubes without containing synaptic vesicles) and the total activity of the [^{3}H] solutions (by directly adding 10 µL to scintillation vials) were measured.

At first, the total volume per tube was 400 µL with 20 µL of synaptic vesicles added (roughly 6 µg of protein). After some experiments and optimising the protocol, the total volume was reduced to 200 µL with 10 µL of vesicles added in order to save material.

2.5.3 Radioligand binding

I also followed a modified protocol, originally described by Dr. Pifl (Pifl et al. 2014). Briefly, binding in synaptic vesicles was performed in 25 mM sodium phosphate (SP) buffer (pH = 7.4) containing [^{3}H]dihydrotetrabenazine (DTBZ) (20 nM). First, in each tube 20 µL of synaptic vesicles were added to 80 µL of SP buffer, containing different concentrations of unlabelled GABA or the inhibitor tetrabenazine, and pre-incubated for 5 min at 30°C. After adding 100 µL of SP buffer with [^{3}H]DTBZ, the reactions were incubated for 90 min at 30°C. Non-specific binding was determined in the presence of 10 µM unlabelled tetrabenazine. The reactions were stopped by adding ice-cold SP buffer to the tubes and then filtered through poly(ethyleneimine)-coated (1% w/v) GF/B glass fiber filters (Whatman).

For the first experiments, the filtration was done using an automated cell harvester filtration device (Skatron Instruments AS). Two of the twelve channels of the Skatron could not be used due to technical issues (blockage), increasing to three channels and at some point all tubes were overflowing before filtration, rendering the filtration device useless for these experiments. From this point on, the filtrations were done the same way as for the uptakes, using 2 mL of ice-cold SP buffer for the washes. The filters were then transferred to scintillation vials, shaken for 1 h and measured in a liquid scintillation counter (PerkinElmer/Revvity). Each binding assay was performed in duplicate determinations. Additionally, a filter blank (treated like all other tubes but without containing synaptic vesicles) and the total activity of the [^{3}H] solutions (by directly adding 100 µL to scintillation vials) were measured.

2.6 FFN206 assays

False fluorescent neurotransmitters (FFNs) are fluorescent substrates for specific transporters that can be used for uptake assays (Gubernator et al. 2009), FFN206 being a substrate for VMAT2 (Hu et al. 2013). The principle is basically the same as when using radiolabelled substrates, but in contrast the handling is much safer and the material is significantly less expensive. Also, e.g. live cell imaging can be achieved using FFNs because for measurement they do not need to be lysed, but are just taken to a plate reader or (epi)fluorescent microscope. Briefly, cells are incubated with special experimental cell culture media in presence and absence of FFN206 and also testing substances (here reserpine/tetrabenazine). After washing the cells, in a plate reader the intensity of the fluorescent signal is measured, which correlates to the amount of taken up FFN206.

2.6.1 Uptake

For the FFN206 experiments I followed and slightly modified the protocol described in (Hu et al. 2013). HEK293 and polyclonal HEK293-VMAT2:eGFP cells were grown in a 96-well plate coated with poly-D-lysine. Prior to uptake, the medium was aspirated and 180 µL of experimental medium (DMEM without phenol red, FBS, penicillin or streptomycin) was added to each well, followed by addition of 10 µL DMSO in experimental medium (vehicle control) or different concentrations of reserpine/tetrabenazine in experimental medium for pre-incubation (30 min at 37°C and 5% CO_2). Then 10 µL of FFN206 solution (final 1 µM) or DMSO (negative control) in experimental medium were added to each well and incubated for 1 h at 37°C and 5% CO_2. After washing the cells with PBS, they were kept in 120 µL PBS and immediately measured on a plate reader (excitation wavelength 340 ± 25 nm, emission wavelength 450 ± 10 nm). All conditions were prepared and measured in triplicates.

2.6.2 Microscopy

HEK293 and polyclonal HEK293-VMAT2:eGFP cells were grown in a 24-well plate coated with poly-D-lysine. After washing with PBS, the cells were pre-incubated in 500 µL experimental medium containing 2 µL DMSO in experimental medium (vehicle control) or reserpine/tetrabenazine in experimental medium (final 4 µM) for 30 min at 37°C and 5% CO_2. Next, 500 µL of FFN206 solution (final 10 µM) or DMSO (negative control) in experimental medium were added to each well and incubated for 1 h at 37°C and 5% CO_2. After washing the cells with PBS, they were kept in 500 µL experimental medium and images were taken at the Nikon epifluorescent microscope at 4x, 10x and 20x, using a DAPI filter for detection of FFN206 and a GFP filter for VMAT2.

2.7 Co-immunoprecipitation and western blot

Co-immunoprecipitation experiments are done to discover possible interactions between proteins. First, a sample containing the proteins of interest is incubated with primary antibodies against one of the proteins, which are then pulled down by adding protein G beads. In this step everything not bound to the antibodies and therefore the protein G beads or closely interacting with the bound proteins is washed away. After elution of all proteins from the protein G beads, they need to be separated from the heterogenous mixture by using sodium dodecyl sulphate polyacrylamide gel electrophoresis (SDS-PAGE). In order to immobilise the proteins afterwards and to make them detectable, they are transferred to a nitrocellulose membrane. After incubation with primary antibodies against the protein(s) of interest, the membranes are incubated with secondary antibodies conjugated to some marker, in this case they are fluorescent for detection of the proteins, and finally imaged.

2.7.1 Cell lysates

Cells were grown in a 10 cm plastic dish, washed twice with ice-cold PBS and lysed in immunoprecipitation (IP) buffer (containing 50 mM Tris-HCl, 150 mM NaCl, 1 mM EDTA, 1% Triton X-100 supplemented with protease inhibitors). The lysate was then transferred to a tube and incubated on a rotator for 30 min at 4°C. After centrifugation for 10 min at 14,000 rpm at 4°C, the supernatant was kept on ice for direct use or stored at -20°C and the protein concentration determined using a BCA Kit (Thermo Fisher Scientific).

2.7.2 Tissue lysates

Mouse hippocampus or striatum were homogenised in ice-cold 0.32 M sucrose containing 25 mM Tris-HCl (pH = 7.4), using a glass Teflon Potter-type homogeniser (20 strokes). The homogenates were then centrifuged for 15 min at 1,000 x g at 4°C and the supernatant was again centrifuged for 30 min at 20,000 x g at 4°C, resulting in a ‘P2’ pellet. The P2 pellet was incubated in IP buffer on a rotator for 60 min at 4°C and the lysate then centrifuged for 10 min at 21,000 x g at 4°C. The supernatant was kept on ice for direct use or stored at -20°C and the protein concentration determined via the BCA assay.

2.7.3 Co-immunoprecipitation

The lysates (volumes containing ca. 200 µg protein) were incubated with primary antibodies (1 µg per 100 µg protein) and incubated on a rotator overnight at 4°C. On the next day, protein G beads were washed with IP buffer thrice for equilibration and then added to the lysates. After 4 h incubation on a rotator at 4°C, the suspensions were washed thrice with IP buffer and after discarding all liquid, the IgG beads were incubated with 2x Laemmli buffer (containing 0.1 M Tris-HCl, 0.14 M SDS, 20% glycerol, 2,5% ß-mercaptoethanol and 1.5 mM bromophenol blue) either for 3 min at 95°C, 15 min at 50°C, 30 min at 37°C or 30 min at room temperature to elute the antibodies from the protein G beads and the eluate was transferred to a new tube, stored at -20°C.

2.7.4 Immunoblotting

Polyacrylamide gels were cast and the lanes loaded with the prepared samples, as well as a protein ladder (Thermo Scientific). A polyacrylamide gel for SDS-PAGE consists of a running gel (10% acryl-bisacrylamide, 1% SDS, 0.375 M Tris pH 8.8, 1% ammonium persulfate (APS) and 6,7 mM tetramethyl ethylenediamine (TEMED)) and a stacking gel (5% acryl-bisacrylamide, 1% SDS, 0,125 M Tris pH 6,8, 1% APS and 6,7 mM TEMED). First the gels were run at 100 V until the loading front reached the running gel (about 15 min), then the voltage was increased to 150 V and the gels run for about another hour.

After rinsing the gels with ddH_2O and equilibrating in transfer buffer (TB) (containing 25 mM Tris-HCl, 192 mM glycine and 10% methanol), proteins were transferred to nitrocellulose membranes (Amersham) via wet transfer for 45 min at 100 V. The membranes were then incubated with Ponceau S staining solution (Sigma, 0.1% Ponceau S in 5% acetic acid) for 1 min, and an image was taken after rinsing briefly with ddH_2O. Afterwards, the membranes were also rinsed with Tris-buffered saline with tween (TBST) (pH 7.5 containing 20 mM Tris-HCl, 150 mM NaCl and 0.1% Tween 20) and then incubated in a 5% non-fat dry milk (NFDM) blocking solution in TBST for 1 h at room temperature.

Then the membranes were incubated with the primary antibody solutions (in TBST) (**Table 3**) overnight at 4°C. On the next day, after washing thrice with PBS the membranes were incubated with IRDye 680-RD-labelled secondary antibodies (LI-COR Biotechnology GmbH) (**Table 3**) in 5% NFDM blocking solution for 2 h at room temperature. When two different primary antibodies were co-labelled, instead of using two secondary antibodies with different detection wavelengths, samples were loaded on the gel in duplicates and the blotted membrane was cut in half. These halves were then incubated separately with different primary antibodies. Finally, the membranes were imaged on the LI-COR Odyssey CLx infrared imaging system and then stored at -20°C.

Table 3: Used antibody solutions for immunoblots.

Antibody	**Brand**	**Identifier**	**Dilution**
Primary antibodies			
Mouse anti-GFP	Santa Cruz	#sc-9996	1:1000
Rabbit anti-GAT1 polyclonal	Synaptic Systems	#274 102	1:1000 or 1:2000
Rabbit anti-VMAT2 polyclonal	Synaptic Systems	#138 313	1:2000
Secondary antibodies			
Goat anti-Mouse IRDye 680RD	LI-COR	#926-68070	1:5000
Goat anti-Rabbit IRDye 680RD	LI-COR	#926-68071	1:5000

2.8 Data analysis

For the synaptic vesicle uptake experiments with [^{3}H]5-HT, the amount of radioactivity measured (counts per minute [cpm]) in the absence of vesicles ('filter blank'; unspecific binding of ^{3}H to the filter) was subtracted from the cpm measured in the presence of vesicles containing either vehicle (control) or test compounds (GABA, reserpine, tetrabenazine, glycine or taurine).

For [^{3}H]GABA uptakes as well as binding experiments, the cpm of non-specific uptake/binding (i.e. the uptake/binding in the presence of inhibitors (reserpine/tetrabenazine)) was subtracted from the cpm measured in vesicles containing vehicle (control) or test compounds (GABA, reserpine, tetrabenazine).

For graphs showing relative values, the average of the uptake/binding cpm obtained per experiment (everything was performed in duplicates) in the presence of vehicle (control) was set to 100% after subtracting the filter blank. Cpm in the presence of test compounds (GABA, reserpine, tetrabenazine, glycine or taurine) are expressed as percentage of control. These graphs show summaries of the mean of the means of all different animals.

Data are also shown after normalization to the protein amount present in each sample. To do so, cpm were converted to either pmol/min/mg protein in case of uptakes or pmol/mg protein for binding. Graphs display means from the duplicate determinations. (Limani et al. 2024)

In case of FFN206 uptake experiments, the measured fluorescent signal is expressed as relative fluorescent units [RFU]. For baseline-corrected data, RFU in absence of FFN206 were subtracted from RFU measured in the presence of vehicle (control) or test compounds (reserpine, tetrabenazine). For graphs showing relative values from baseline-corrected data, FFN206 uptake in absence of other compounds was set to 100%. Everything was measured in triplicates.

Data analysis and graphs were done in GraphPad Prism (GraphPad Software Inc., San Diego, CA), all data are expressed as means ± SEM. Microscope images were edited using Fiji/ImageJ (NIH, open source).

3 Rationale and working hypothesis of this thesis

It is known that midbrain dopamine (DA) neurons can co-release DA and glutamate. Although there is data indicating that γ-aminobutyric acid (GABA) can also be co-released from DA neurons, the underlying mechanism is not entirely clear since DA neurons lack the machinery for the canonical pathway of GABA synthesis and release (Melani and Tritsch 2022). The work of Tritsch et al. shows that GABA co-release is dependent on the vesicular monoamine transporter VMAT2 for vesicular packaging (Tritsch et al. 2012). While the data is very convincing, they indirectly measured inhibitory postsynaptic currents at $GABA_A$ receptors in striatal neurons, meaning that theoretically those currents could also have been evoked by other $GABA_A$ receptor ligands like glycine and taurine (Jonas et al. 1998). Most importantly, GABA is structurally very different to the classical VMAT2 substates (which are monoamines) and would therefore represent a rather unconventional VMAT2 substrate.

Therefore, I wanted to perform radiotracer flux/binding measurements in synaptic vesicles isolated from the brains of different species, to see whether GABA is indeed a substrate for VMAT2. I started with uptake of [^{3}H]5-HT, a VMAT2 substrate, and addition of different GABA concentrations to see if the uptake could be reduced. Next, I did binding assays with [^{3}H]dihydrotetrabenazine (DTBZ) to test if GABA could displace a high affinity inhibitor of VMAT2. Finally, I also tried to measure [^{3}H]GABA uptake in synaptic vesicles directly, since this would prove best if GABA is indeed a VMAT2 substrate.

After performing uptake assays with radiolabelled compounds, I also wanted to try an assay utilising a fluorescent substrate for VMAT2, the fluorescent false neurotransmitter FFN206, as an alternate approach to confirm the above findings. This is of high interest because the handling is safer compared to radioactive material, it is less expensive and could even be used for live cell imaging. Since the data in the original paper was acquired using HEK293 and stable HEK293-VMAT2 cells (Hu et al. 2013), I first wanted to see whether I could replicate them and so I also performed the experiments in HEK cells stably expressing human VMAT2.

Since the relative affinity of GABA is very low even at the vesicular GABA transporter (VGAT) (McIntire et al. 1997), I speculate that VMAT2 has an equally low or even lower affinity. This would mean that for GABA to be transported by VMAT2 at physiologically meaningful rates, local GABA concentrations would have to be relatively high (at least in the millimolar range). One possibility to enable efficient transport could be a close interaction between VMAT2 and the GABA transporter GAT1, that imports GABA from outside the cell. To test if there might be such an interaction, I started to perform co-immunoprecipitations to determine whether the two proteins would co-purify.

4 Results and discussion

4.1 Radioligand uptakes

First, it was tested in mouse synaptic vesicles from the striatum, whether our vesicular uptake assay itself is robust and if a K_M for serotonin (5-HT) at VMAT2 similar to literature values can be obtained. In order to achieve that, a saturation uptake assay with different serotonin concentrations was performed, showing an apparent K_M of 171 nM (**Figure 5**). Compared to literature values like 290 nM (Finn and Edwards 1997), this was considered reasonable and a confirmation of assay feasibility.

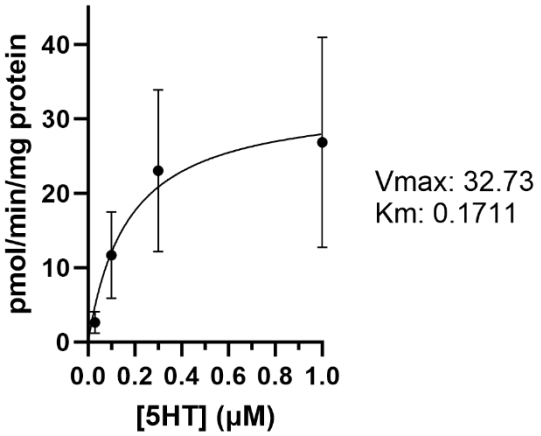

Figure 5: The utilized uptake assay in synaptic vesicles is a robust assay. Saturation uptake of [^{3}H]5-HT in mouse striatal synaptic vesicles (n=4) yielded a K_M of about 171 nM. Data points were measured at 0.03, 0.1, 0.3 and 1 µM 5-HT and the cpm values normalised to [pmol/min/mg protein]. Incubation time was 5 min at 30°C.

Next, it was tested whether addition of non-labelled GABA at different concentrations would affect [^{3}H]5-HT uptake through VMAT2, which is expected if VMAT2 can indeed transport GABA and provided GABA has an overlapping binding site with monoamines.

For that purpose, I performed radiotracer flux measurements, where I isolated synaptic vesicles from striatum or cerebellum of mouse brains and incubated them with radiolabelled serotonin ([^{3}H]5-HT), a substrate at VMAT2, under different conditions. Uptake of [^{3}H]5-HT in the presence or absence of different concentrations of GABA was measured. The VMAT2-specific inhibitor reserpine was used at a saturating concentration (2 µM) to define VMAT2-specific uptake (also termed non-specific uptake). After stopping the uptake with ice-cold buffer, the amount of [^{3}H]5-HT taken up into synaptic vesicles was determined by measuring the amount of radioactivity present on filters via liquid scintillation spectroscopy.

From the results it can be concluded that firstly, GABA concentration-dependently decreased [^{3}H]5-HT uptake at VMAT2 and secondly, that the inhibitory effect of GABA at VMAT2 is rather weak (**Figure 6**). Because of baseline differences between individual experiments, the summarised relative values were normalised to control ([^{3}H] uptake without adding a test compound; dotted line in the graphs). Only at relatively high GABA concentrations, starting at around 10 mM, did I observe a decrease in [^{3}H]5-HT uptake. Interestingly, while intracellular monoamine concentrations are typically in the micromolar range, intracellular GABA levels (as well as glutamate) are assumed to be in the millimolar range (Edwards 2007). Hence, it is conceivable that uptake of GABA via VMAT2 is physiologically possible.

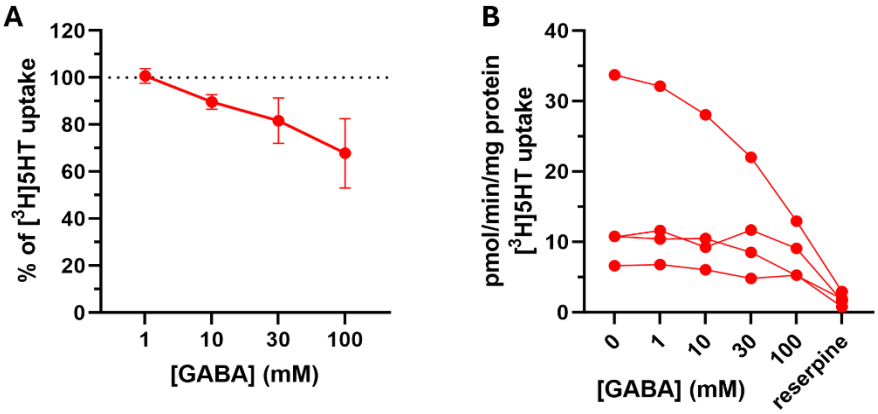

Figure 6: GABA decreased uptake of 5-HT in mouse synaptic vesicles. (A) *GABA concentration-dependently decreased [^{3}H]5-HT uptake in mouse striatal synaptic vesicles (n=4). Summarised data is shown as % of [^{3}H]5-HT uptake after adding 1, 10, 30 and 100 mM of GABA.* ***(B)*** *Data of individual uptake experiments is shown, measured cpm values were normalised to [pmol/min/mg protein] of [^{3}H]5-HT uptake. Tested conditions were [^{3}H]5-HT uptake after addition of 0, 1, 10, 30 and 100 mM of GABA or 2 µM of reserpine (non-specific uptake). Radioligand concentration was 100 nM, incubation with [^{3}H]5-HT was 5 min at 30°C.*

After seeing these results, the question was if a similar concentration-dependent decrease of [^{3}H]5-HT uptake could also be observed in striatal synaptic vesicles isolated from other species and hence whether this effect was evolutionarily conserved.

I therefore tested rat (**Figure 7**) and monkey (**Figure 8**) striatum. Indeed, similar effects were seen in rat and monkey synaptic vesicle uptakes, supporting a weak decrease of [^{3}H]5-HT uptake at millimolar GABA concentrations.

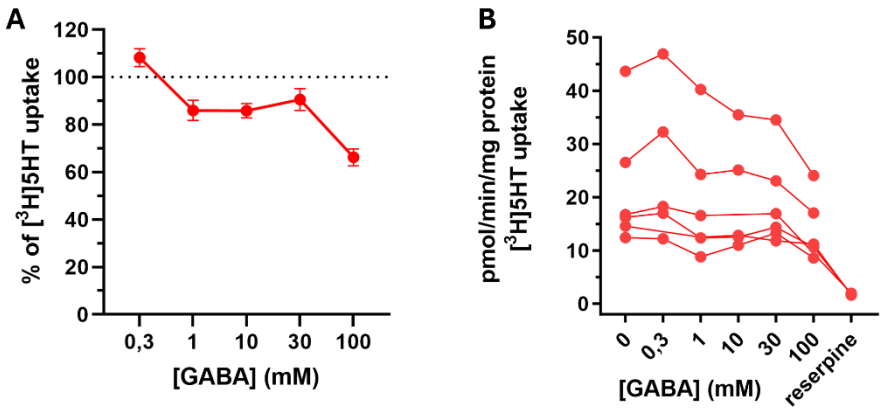

Figure 7*: GABA decreased uptake of 5-HT in rat synaptic vesicles.** ***(A) *GABA concentration-dependently decreased [^{3}H]5-HT uptake in rat striatal synaptic vesicles (n=4-6). Summarised data is shown as % of [^{3}H]5-HT uptake after adding 0.3, 1, 10, 30 and 100 mM of GABA.* ***(B)*** *Data of individual uptake experiments is shown, measured cpm values were normalised to [pmol/min/mg protein] of [^{3}H]5-HT uptake. Tested conditions were [^{3}H]5-HT uptake after addition of 0, 0.3, 1, 10, 30 and 100 mM of GABA or 2 µM of reserpine (non-specific uptake). Radioligand concentration was 100 nM, incubation with [^{3}H]5-HT was 5 min at 30°C.*

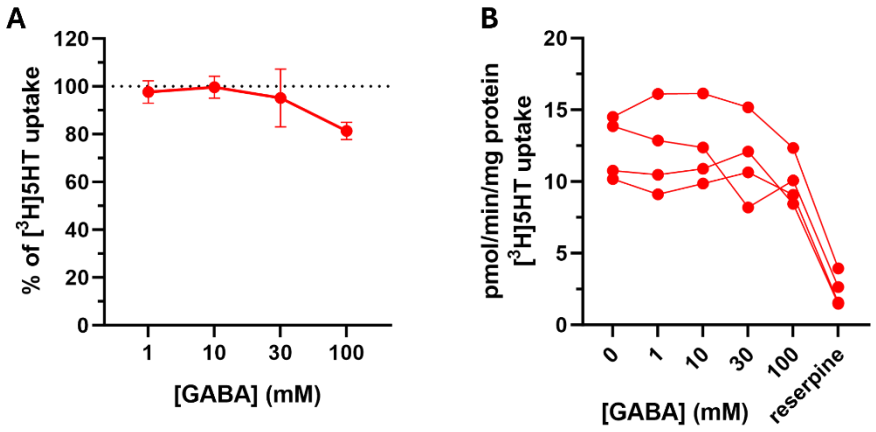

Figure 8: GABA decreased uptake of 5-HT in monkey synaptic vesicles. ***(A)*** *GABA concentration-dependently decreased [^{3}H]5-HT uptake in monkey striatal synaptic vesicles (n=4). Summarised data is shown as % of [^{3}H]5-HT uptake after adding 1, 10, 30 and 100 mM of GABA.* ***(B)*** *Data of individual uptake experiments is shown, measured cpm values were normalised to [pmol/min/mg protein] of [^{3}H]5-HT uptake. Tested conditions were [^{3}H]5-HT uptake after addition of 0, 1, 10, 30 and 100 mM of GABA or 2 µM of reserpine (non-specific uptake). Radioligand concentration was 100 nM, incubation with [^{3}H]5-HT was 5 min at 30°C.*

Similar to the first uptakes in mouse striatum (**Figure 6**), uptakes were also performed in mouse cerebellum to see whether VMAT2 is GABA-sensitive in a brain area, that derives monoamine inputs primarily from serotonergic and noradrenergic areas instead of DAergic (**Figure 9**). Interestingly, the results were almost identical to uptake in striatal synaptic vesicles, confirming a decrease of [^{3}H]5-HT at millimolar GABA concentrations. Again, this supports the idea that GABA is a weak substrate at VMAT2.

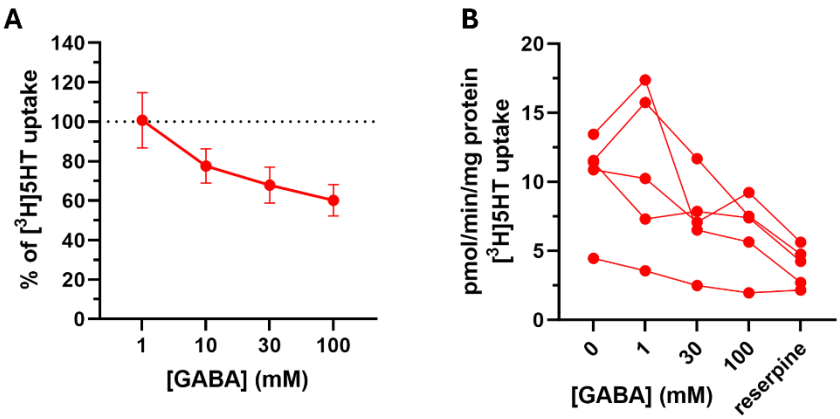

Figure 9: GABA decreased uptake of 5-HT in mouse synaptic vesicles. (A) *GABA concentration-dependently decreased [^{3}H]5-HT uptake in mouse cerebellar synaptic vesicles (n=5). Summarised data is shown as % of [^{3}H]5-HT uptake after adding 1, 10, 30 and 100 mM of GABA.* ***(B)*** *Data of individual uptake experiments is shown, measured cpm values were normalised to [pmol/min/mg protein] of [^{3}H]5-HT uptake. Tested conditions were [^{3}H]5-HT uptake after addition of 0, 1, 10, 30 and 100 mM of GABA or 2 µM of reserpine (non-specific uptake). Radioligand concentration was 100 nM, incubation with [^{3}H]5-HT was 5 min at 30°C.*

Of course, we were also interested in whether we could observe this effect on [^{3}H]5-HT uptake in human striatal synaptic vesicles as well. To test this, synaptic vesicles were isolated from frozen postmortem human striatum (nucleus caudatus) (**Figure 10**)**.** Our experience with human frozen samples has shown in the past that roughly 50% of human tissue is still usable for uptake experiments, which was also found in these preliminary uptakes. Compared to tissue from laboratory animals, assay feasibility is a much bigger problem in human postmortem tissue because of differences in postmortem interval, freezing conditions etc. (Stan et al. 2006).

Also, because we had only very limited human brain tissue available, we tested only one concentration of GABA (30 mM) (**Figure 10**). If all necessary compounds for uptake assays are still intact, one would expect [^{3}H]5-HT uptake to yield the highest cpm measured while there should be some decrease in uptake after adding 30 mM of GABA and even more after adding 2 µM reserpine (if VMAT2-sensitive) (**Figure 10**).

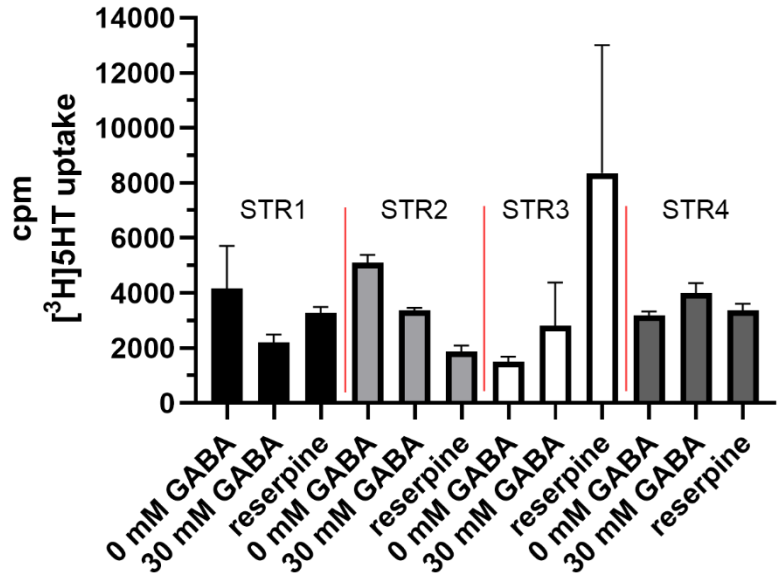

Figure 10: Uptake data from human synaptic vesicles (nucleus caudatus) showed high variability. *Cpm measured from [^{3}H]5-HT uptakes of four representative experiments (STR1-4) are shown. Tested conditions were [^{3}H]5-HT uptake after addition of 0 and 30 mM of GABA or 2 µM of reserpine (non-specific uptake). Radioligand concentration was 100 nM, incubation with [^{3}H]5-HT was 5 min at 30°C.*

As already discussed, GABA is an amino acid and therefore structurally as well as physicochemically different compared to typical VMAT2 substrates, which are monoamines. The pKa of GABA is around 7 (Krishek et al. 1996; Rodrigo et al. 2017), while the pKa for serotonin and dopamine is around 10 (Pratuangdejkul et al. 2006; Armstrong and Barlow 1976). This means that under physiological conditions, GABA has no net charge (but is present as a 'zwitterion') whereas the typical neurotransmitters transported by VMAT2 are all positively charged. Of course, this could influence the uptake and might be one explanation for the low affinity of GABA, or may require different gradients than needed for uptake of cationic monoamines.

Uptake of monoamine substrates at VMAT2 is pH-dependent. Hence, [^{3}H]5-HT uptakes in presence and absence (controls) of unlabelled GABA were performed at three different pH levels (**Figure 11**) to see if there is any pH-dependency in the interaction of GABA with VMAT2. What can be concluded from the results (**Figure 11**) is that uptake at VMAT2 decreased at lower pH (6.8), as expected due to a lower pH-gradient (inside vesicles the pH is around 5.5) (Edwards 2007) and increased at higher pH (8.0) due to a higher pH-gradient. The uptake with addition of 30 mM GABA stayed almost the same relative to the control (almost parallel curves), indicating that the inhibitory effect of GABA did change proportionally to [^{3}H]5-HT uptake with varying pH.

I would have expected a stronger decrease of [^{3}H]5-HT uptake with GABA compared to control at lower pH, since the proportion of the cationic GABA species should increase at lower pH and that would presumably better resemble a typical VMAT2 substrate (see pKa values in this section after human uptakes graph).

In contrast, at higher pH more of the anionic GABA species would be expected, which may cause smaller inhibitory effects of GABA on [^{3}H]5-HT uptake. While my experiments show no significant effects of pH, it must also be mentioned that only a small range from pH 6.8 to 8.0 was tested. Most likely, the positive and negative ionic species of GABA did not change sufficiently to influence uptake, because in this range almost the whole GABA population is present in its zwitterionic form without a net charge (see **Figure 2**). As shown in the introduction (**Figure 2**), only at around pH 3.5 half of the GABA molecules will be positively charged and around pH 10.5 half will be negatively charged (Krishek et al. 1996). Unfortunately, it is not possible to perform this experiment in these pH ranges, since at pH 5.5 and below there is no proton gradient left for transport of [^{3}H]5-HT via VMAT2 and on the other hand, a pH too high would most likely damage the synaptic vesicles and maybe also other components. Physiologically, pH values high enough for GABA to have a positive net charge might still be possible through microdomains, where the pH could vary locally *in vivo* (Ro and Carson 2004) and enhance uptake of GABA at VMAT2, which we would not see in the utilised radiotracer flux measurements.

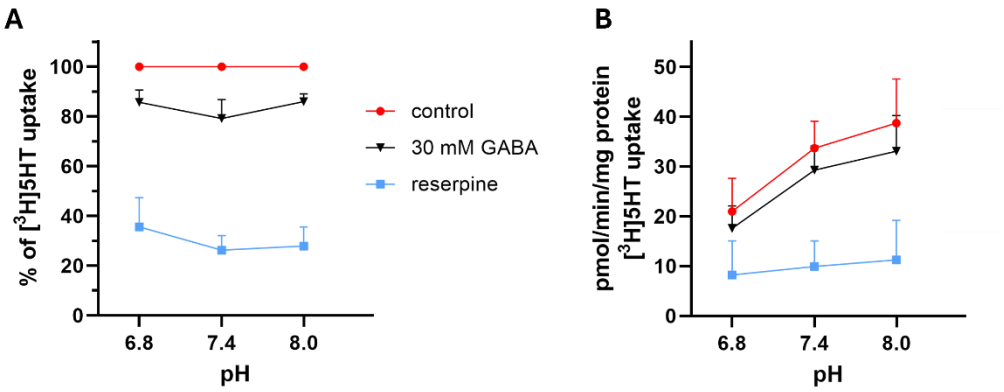

Figure 11: Varying pH did not seem to alter inhibitory effects of GABA on 5-HT uptake. (A) *Increasing pH increased [^{3}H]5-HT uptake in mouse striatal synaptic vesicles (n=5) but did not considerably affect relative decrease in uptake after adding 30 mM GABA. Summarised data is shown as % of [^{3}H]5-HT uptake after adding 0 and 30 mM of GABA or 2 µM reserpine.* ***(B)*** *Summarised data is shown, measured cpm values were normalised to [pmol/min/mg protein] of [^{3}H]5-HT uptake. Tested conditions were [^{3}H]5-HT uptake after addition of 0 and 30 mM GABA or 2 µM reserpine (non-specific uptake) at pH 6.8, 7.4 and 8.0. Radioligand concentration was 100 nM, incubation with [^{3}H]5-HT was 5 min at 30°C.*

Next, also other $GABA_A$ receptor ligands were tested as possible VMAT2 substrates, i.e. glycine (**Figure 12**) and taurine (**Figure 13**). This was of interest because as mentioned in the introduction, until now GABA was shown to be a substrate for VMAT2 only indirectly by measuring postsynaptic inhibitory currents at $GABA_A$ receptors. In the experiments performed by Tritsch et al., they introduced channelrhodopsin 2 to midbrain DA neurons to optically induce neurotransmitter release through blue light flashes. Then they utilised the patch-clamp technique on striatal neurons to measure induced postsynaptic inhibitory currents at $GABA_A$ receptors. They concluded that GABA was responsible for the currents measured since it is the main agonist at $GABA_A$ receptors (Melani and Tritsch 2022), but there could also be other $GABA_A$ receptor ligands like glycine and taurine that could have caused IPSCs through $GABA_A$ receptors (Jonas et al. 1998; Meera et al. 2023). What can be seen in the following graphs is that glycine did not seem to effect [^{3}H]5-HT uptake at all (**Figure 12**), while increasing concentrations of taurine had similar effects at decreasing [^{3}H]5-HT uptake like GABA (**Figure 13**). This indicates that taurine could also be packaged into vesicles by VMAT2 and be responsible for postsynaptic currents at $GABA_A$ receptors.

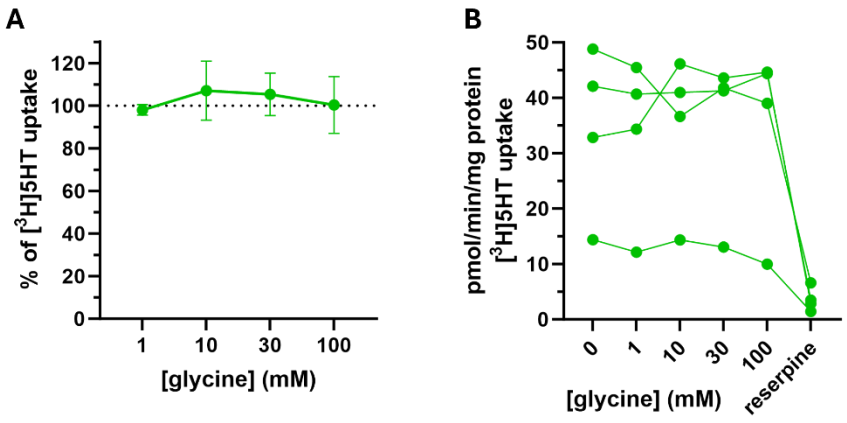

Figure 12: Glycine did not decrease uptake of 5-HT in mouse synaptic vesicles. ***(A)*** *Glycine did not concentration-dependently decrease [^{3}H]5-HT uptake in mouse striatal synaptic vesicles (n=4). Summarised data is shown as % of [^{3}H]5-HT uptake after adding 1, 10, 30 and 100 mM of GABA.* ***(B)*** *Data of individual uptake experiments is shown, measured cpm values were normalised to [pmol/min/mg protein] of [^{3}H]5-HT uptake. Tested conditions were [^{3}H]5-HT uptake after addition of 0, 1, 10, 30 and 100 mM of GABA or 2 µM of reserpine (non-specific uptake). Radioligand concentration was 100 nM, incubation with [^{3}H]5-HT was 5 min at 30°C.*

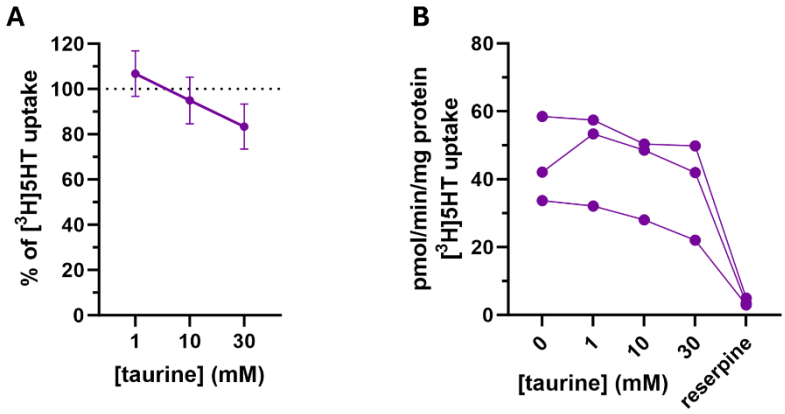

Figure 13: Taurine decreased uptake of 5-HT in mouse synaptic vesicles. ***(A)*** *Taurine concentration-dependently decreased [^{3}H]5-HT uptake in mouse striatal synaptic vesicles (n=3). Summarised data is shown as % of [^{3}H]5-HT uptake after adding 1, 10 and 30 mM of GABA.* ***(B)*** *Data of individual uptake experiments is shown, measured cpm values were normalised to [pmol/min/mg protein] of [^{3}H]5-HT uptake. Tested conditions were [^{3}H]5-HT uptake after addition of 0, 1, 10, and 30 mM of GABA or 2 µM of reserpine (non-specific uptake). Radioligand concentration was 100 nM, incubation with [^{3}H]5-HT was 5 min at 30°C.*

Of course, all uptakes performed so far with [^{3}H]5-HT and addition of different concentrations of non-labelled GABA did not allow to conclude whether GABA itself is a substrate of VMAT2. Only uptake of [^{3}H]GABA would be direct evidence whether GABA is indeed taken up by VMAT2 or not. Since synaptic vesicles containing VGAT are present throughout the brain (Chaudhry et al. 1998), a preparation of striatal synaptic vesicles would always measure uptake of [^{3}H]GABA via VGAT at the same time. Accordingly, whether any [^{3}H]GABA is also transported by VMAT2 is not straightforward to measure, but would strongly be proposed if the addition of VMAT2 blockers like reserpine or TBZ were to block the [^{3}H]GABA uptake. Therefore, uptake of [^{3}H]GABA via VGAT is considered a positive control for GABA uptake, while addition of 30 mM GABA should completely abolish uptake at VGAT (according to (McIntire et al. 1997)) and theoretically should also affect VMAT2-mediated uptake of [^{3}H]GABA. On the other hand, addition of reserpine or tetrabenazine would possibly only affect VMAT2-mediated uptake, but not VGAT-mediated uptake of [^{3}H]GABA.

Unfortunately, the results from synaptic vesicle uptakes in mouse (**Figure 14**) and rat (**Figure 15**) striatum underline the difficulty of measuring [^{3}H]GABA uptake at all (also at VGAT), presumably because the affinity of GABA is very low. Above all, these results cannot be used for any conclusions yet, because the positive and negative controls did not work reliably. One would assume the highest cpm for the control ([^{3}H]GABA uptake in the absence of an inhibitor) and after the addition of 40 µM non-labelled GABA (this would be expected to increase the cpm because of a shift closer to the K_M at VGAT and VMAT2 and hence an increase in velocity), increasing uptake rate of [^{3}H]GABA. In contrast, addition of 30 mM of non-labelled GABA should decrease [^{3}H]GABA uptake because of saturation. This was used as negative control, since uptake via VGAT now was completely blocked. Addition of reserpine or TBZ would be expected to block [^{3}H]GABA uptake when transported by VMAT2. For the uptakes seen in **Figures 14 and 15**, these trends cannot be observed but it is variable and not reproducible. One reason for encountering difficulties when trying to measure [^{3}H]GABA uptake might be the very low relative affinity at VMAT2 and VGAT itself; although not known, the K_M is most likely in the higher millimolar range, since even at VGAT, the main transporter to package GABA into synaptic vesicles, the K_M of GABA is around 5 mM (McIntire et al. 1997).

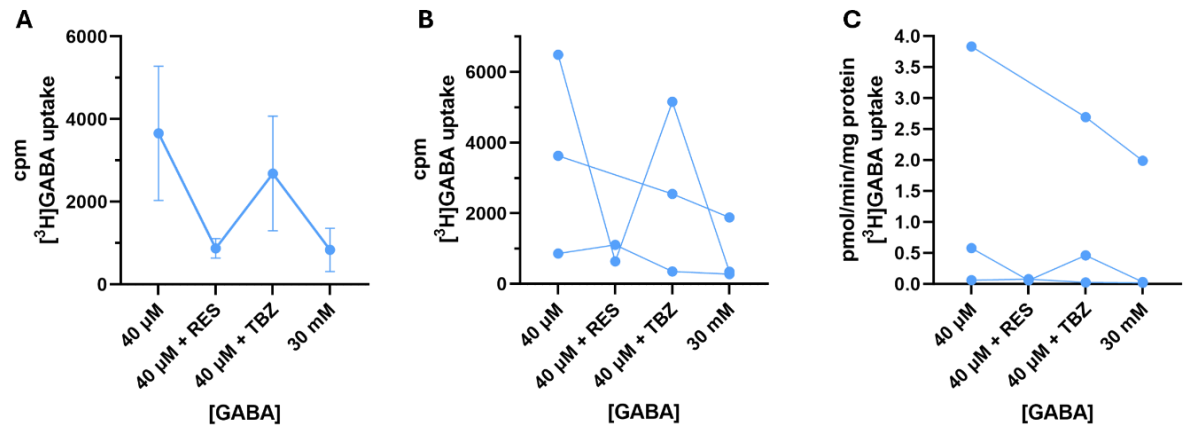

***Figure 14*: GABA uptake was difficult to measure in mouse synaptic vesicles. (A)** *[^{3}H]GABA uptake in mouse striatal synaptic vesicles (n=3). Summarised data is shown as cpm of [^{3}H]GABA uptake after adding 40 µM and 30 mM of GABA or 40 µM of GABA together with 10 µM reserpine/tetrabenazine.* **(B)** *Data if individual experiments is shown as cpm.* **(C)** *Data of individual uptake experiments is shown, measured cpm values were normalised to [pmol/min/mg protein] of [^{3}H]GABA uptake. Tested conditions were [^{3}H]GABA uptake with 40 µM non-labelled GABA (positive control), after addition of 10 µM of reserpine/ tetrabenazine (non-specific uptake) or adding 30 mM non-labelled GABA (negative control). Radioligand concentration was 50 nM, incubation with [^{3}H]GABA 15 min at 30°C.*

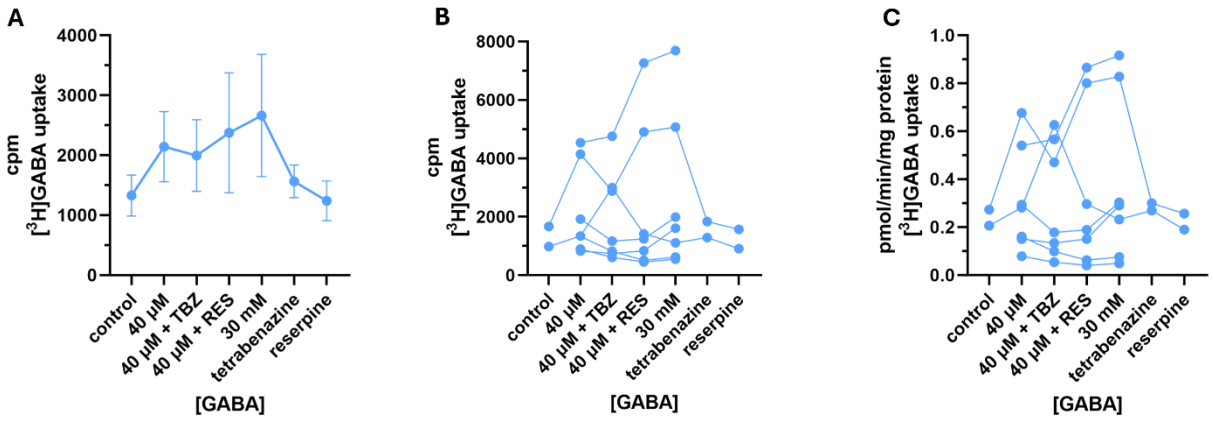

Figure 15: GABA uptake was difficult to measure in rat synaptic vesicles. (A) *[^{3}H]GABA uptake in rat striatal synaptic vesicles (n=2-7). Summarised data is shown as cpm of [^{3}H]GABA uptake only or after adding 40 µM and 30 mM of GABA or 40 µM of GABA together with 10 µM reserpine/tetrabenazine or 10 µM of reserpine/ tetrabenazine only.* **(B)** *Data of individual experiments is shown as cpm.* **(C)** *Data of individual uptake experiments is shown, measured cpm values were normalised to [pmol/min/mg protein] of [^{3}H]GABA uptake. Tested conditions were [^{3}H]GABA uptake alone or with 40 µM non-labelled GABA (positive control), after addition of 10 µM of reserpine/ tetrabenazine with or without 40 µM non-labelled GABA (non-specific uptake) or adding 30 mM non-labelled GABA (negative control). Radioligand concentration was 50 nM, incubation with [^{3}H]GABA was 15 min at 30°C.*

In an attempt to yield clearer results, another more concentrated stock of [^{3}H]GABA was purchased and the uptake experiments were repeated in mouse synaptic vesicles (**Figure 16**). This new [^{3}H]GABA stock had a higher specific activity, meaning that in the same volume there are more GABA molecules labelled with the radioisotope, which theoretically should lead to a better signal-to-noise ratio. Using (final) concentrations of [^{3}H]GABA near the apparent K_M at VGAT and VMAT2 would be best for clear results, so this more concentrated stock could be important because of the low affinity of GABA at VGAT and VMAT2. Despite the higher concentration of [^{3}H]GABA (344 nM instead of 50 nM previously), it was still below millimolar range and as can be seen, the results again were too variable and controls have not yielded clear results, i.e. uptake was not blocked by 30 mM GABA or enhanced by 40 µM GABA as would be expected for GABA-mediated uptake via VGAT. To be able to reliably measure uptake of [^{3}H]GABA, probably even higher concentrations would be needed and maybe even other parameters would have to be changed, like the contents and concentrations of the uptake buffer ingredients, or more concentrated vesicle preparations would need to be used.

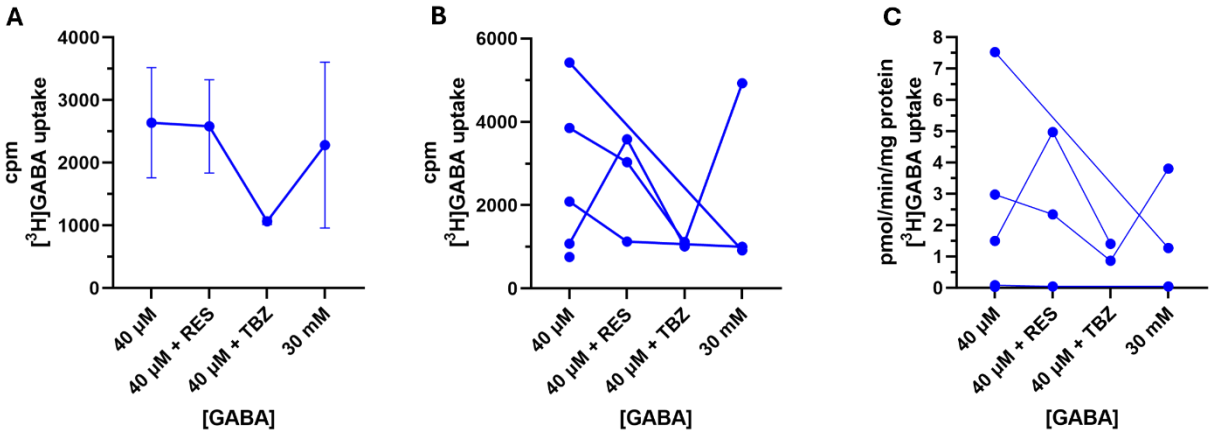

Figure 16: More concentrated GABA uptake was difficult to measure in mouse synaptic vesicles. (A) *[^{3}H]GABA uptake in mouse striatal synaptic vesicles (n=3). Summarised data is shown as cpm of [^{3}H]GABA uptake after adding 40 µM and 30 mM of GABA or 40 µM of GABA together with 10 µM reserpine/ tetrabenazine.* ***(B)*** *Data of individual experiments is shown as cpm* ***(C)*** *Data of individual uptake experiments is shown, measured cpm values were normalised to [pmol/min/mg protein] of [^{3}H]GABA uptake. Tested conditions were [^{3}H]GABA uptake with 40 µM non-labelled GABA (positive control), after addition of 10 µM of reserpine/ tetrabenazine (non-specific uptake) or adding 30 mM non-labelled GABA (negative control). Radioligand concentration was 344 nM, incubation with [^{3}H]GABA was 10 min at 30°C.*

4.2 Radioligand bindings

First, it was tested in mouse synaptic vesicles from the striatum, whether our binding assay is robust and if a K_D for [^{3}H]DTBZ at VMAT2 similar to the literature can be obtained. In order to achieve that, a saturation binding assay with different [^{3}H]DTBZ concentrations was performed, yielding an apparent K_D of 5 nM (**Figure 17**). Compared to literature values like 18 nM (Dalton et al. 2024), this was considered reasonable and supports assay feasibility.

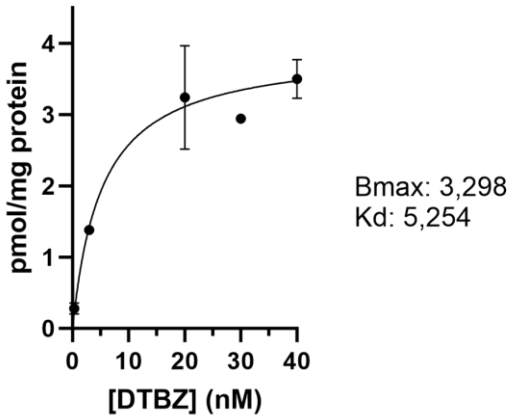

Figure 17: The utilized binding assay in synaptic vesicles worked robustly. *Saturation binding of [^{3}H]DTBZ in mouse striatal synaptic vesicles (n=3) yielded a K_D of about 5 nM. Data points were measured at 0.3, 3, 20, 30 and 40 nM DTBZ and the cpm values were normalized to [pmol/mg protein]. Incubation with [^{3}H]DTBZ was 90 min at 30°C.*

Next, it was tested whether GABA would be able to displace [^{3}H]DTBZ, which is a close analogue (the keto group in the piperidin ring is reduced to a hydroxyl group) to the high-affinity VMAT2 ligand tetrabenazine. The results from these binding assays show that binding of [^{3}H]DTBZ was not affected even at the highest GABA concentrations used, neither in mouse (**Figure 18**) nor in rat (**Figure 19**) striatal synaptic vesicles. One explanation could be the vast difference in affinity of several orders of magnitudes between the antagonist DTBZ (low nanomolar range) (Wang et al. 2024) and the putative substrate GABA (millimolar range) and a presumably much lower off-rate (k_{off}) of DTBZ compared to GABA. In contrast, the affinity of monoamines towards VMAT2 is in the micromolar range (Finn and Edwards 1997) and my therefore be easier to displace by a low-affinity substrate such as GABA. Interestingly, since the binding sites of 5-HT and TBZ are overlapping at VMAT2 (Pidathala et al. 2023; Wang et al. 2024), it may seem likely that the binding sites of TBZ and GABA also overlap.

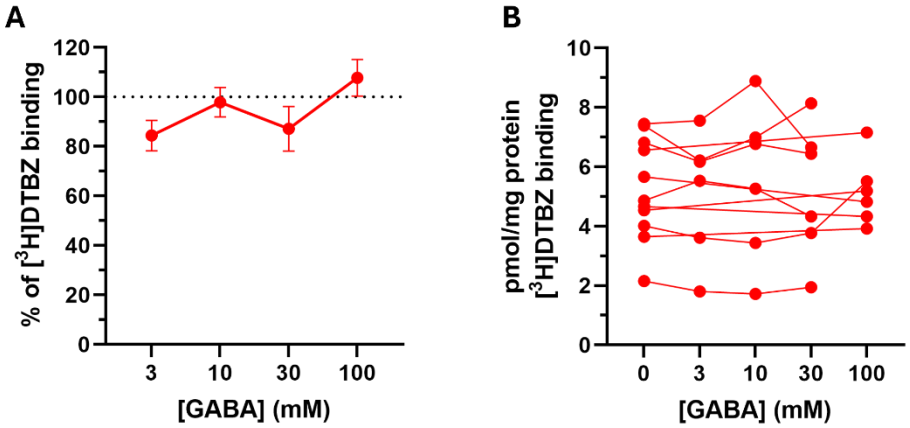

Figure 18: GABA did not decrease binding of DTBZ in mouse synaptic vesicles. (A) *Binding of [^{3}H]DTBZ were not affected in mouse striatal synaptic vesicles (n=5-6). Summarised data is shown as % of [^{3}H]DTBZ binding after adding 3, 10, 30 and 100 mM of GABA.* ***(B)*** *Data of individual binding experiments is shown, measured cpm values were normalised to [pmol/mg protein] of [^{3}H]DTBZ binding. Tested conditions were [^{3}H]DTBZ binding after addition of 0, 3, 10, 30 and 100 mM of GABA or 10 µM of tetrabenazine (non-specific binding, not shown). Radioligand concentration was 20 nM, incubation with [^{3}H]DTBZ was 90 min at 30°C.*

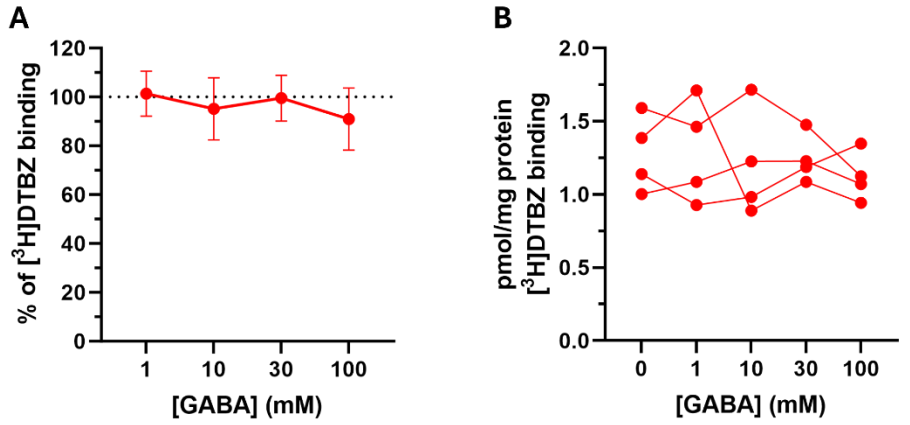

Figure 19: GABA did not decrease binding of DTBZ in rat synaptic vesicles. (A) *Binding of [^{3}H]DTBZ was not affected in rat striatal synaptic vesicles (n=4). Summarised data is shown as % of [^{3}H]DTBZ binding after adding 1, 10, 30 and 100 mM of GABA.* ***(B)*** *Data of individual binding experiments is shown, measured cpm values were normalised to [pmol/mg protein] of [^{3}H]DTBZ binding. Tested conditions were [^{3}H]DTBZ binding after addition of 0, 1, 10, 30 and 100 mM of GABA or 10 µM of tetrabenazine (non-specific binding, not shown). Radioligand concentration was 20 nM, incubation with [^{3}H]DTBZ was 90 min at 30°C.*

4.3 FFN206

The fluorescent false neurotransmitters (FFNs) are a group of neurotransmitters, that are analogues of various transporter substrates. Many are substrates at VMAT2 and initially they were developed to observe neurotransmitter uptake and release from individual presynaptic terminals (Gubernator et al. 2009). They do not need an additional tag, since they are fluorescent because of their aromatic rings/ conjugated electronic system (see **Figure 20**) (Alvarez et al. 2011). Here, FFN206 was used, which has been found to be a specific substrate at VMAT2 (Hu et al. 2013). Conducting uptake assays with FFN206 instead of radiotracers would be of much interest, because the handling and disposal is safer (no radioactivity), FFN206 is a lot cheaper than e.g. [^{3}H]5-HT, this assays enables VMAT2 monitoring in intact cells/tissues with subcellular spatial resolution and can be used as a high-throughput assay by straightforward and rapid fluorometric measurements (Hu et al. 2013).

***Figure 20: Fluorescent false neurotransmitter 206 (FFN206)**. The VMAT2 substrate FFN206 (like all FFNs) consists of an aromatic conjugated electronic system, causing fluorescence. The figure was taken from (Hu et al. 2013).*

Therefore, experiments were conducted in untransfected HEK293 cells (negative control) and stably transfected HEK293-VMAT2 similar to the first published paper on FFN206 (Hu et al. 2013).

According to the published protocols, there were two differently prepared well plates used, one for microscopy and one for an uptake assay followed by a read-out in a plate reader (PerkinElmer multilabel counter). Since VMAT2 is GFP-labelled, it was also examined whether there would be overlaps in excitation or emission wavelengths with FFN206; excitation wavelengths are 369 nm (FFN206) and 489 nm (eGFP), emission wavelengths are 464 nm (FFN206) and 508 nm (eGFP) (Hu et al. 2013; Patterson et al. 2001). With the chosen wavelengths on the plate reader (λ_{Ex}= 340 ± 25 nm, λ_{Em}= 450 ± 10 nm), there were no interferences to be expected.

At first, an experiment was conducted in order to get a first impression whether these uptake experiments work in general and to find out what measuring conditions might be most suitable. Here, mainly different measuring positions (distance from the bottom of the wells) were tested, as can be seen in the summary (**Figure 21**). At first, the uptake seems to generally have been successful, because uptake of FFN206 could be blocked by adding reserpine or tetrabenazine and was then in the same range as the negative control without FFN206 added. On the other hand, the signal ratio of positive/negative control was comparatively low with only about 15,000 relative fluorescence units (RFU) difference between positive and negative control (**Figure 22 A**) in a range of approximately 50,000 RFU (**Figure 21**). In other words, the measured signal of the negative control was still around 70% of the positive control. This might be due to autofluorescence from the cells or suboptimal measuring conditions. However, after subtracting the negative control (baseline), the non-specific uptake after addition of inhibitors (reserpine/tetrabenazine) went down to about 15% of total FFN206 uptake (**Figure 22 B**), which is comparable to what I have determined in uptake assays using [^{3}H]5-HT in synaptic vesicles.

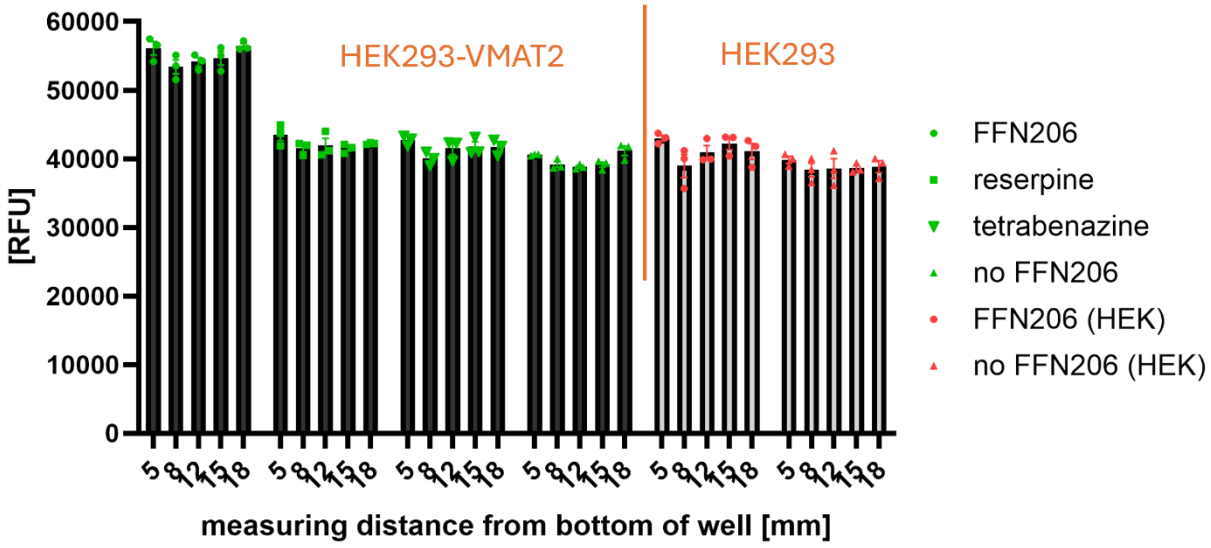

Figure 21: FFN206 uptake in HEK293-VMAT2 cells. *Uptake of FFN206 was measured at different distances (5, 8, 12, 15 and 18 mm) from the bottom of wells of a 96-well plate, using untransfected HEK293 cells as well as stably transfected HEK293-VMAT2 cells. Testing conditions were incubation with FFN206 only, FFN206 + reserpine/tetrabenazine (10 µM) and incubation without FFN206. FFN206 concentration is 1 µM, pre-incubation time was 30 min and incubation with FFN206 was 60 min at 37°C.*

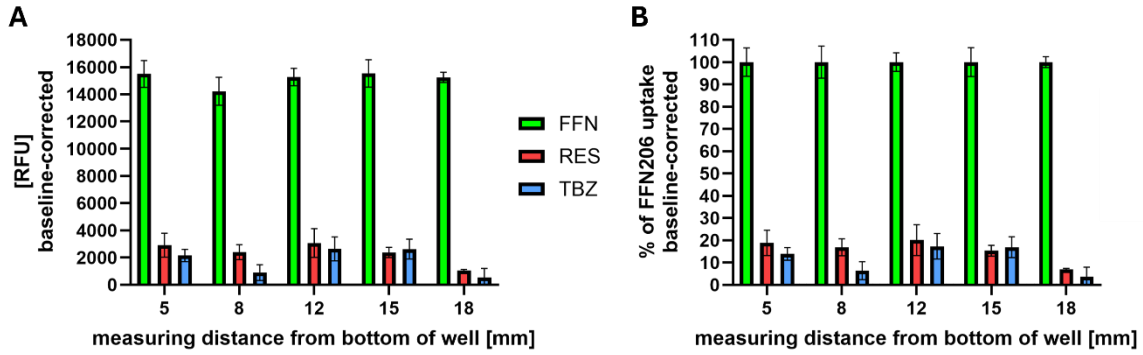

***Figure 22*: Baseline-corrected FFN206 uptake in HEK293-VMAT2 cells.** *Uptake of FFN206 was measured at different distances (5, 8, 12, 15 and 18 mm) from the bottom of wells of a 96-well plate, using a stable HEK293-VMAT2 cell line. Testing conditions were incubation with FFN206 only, FFN206 + reserpine/tetrabenazine (10 µM) and incubation without FFN206 (baseline). Results are shown after subtracting the baseline as RFU **(A)** and as % of FFN206 uptake **(B)**. FFN206 concentration was 1 µM, pre-incubation time was 30 min and incubation with FFN206 was 60 min at 37°C.*

I also performed fluorescent microscopy in parallel to the plate reader measurements to test whether uptake of FFN206 or inhibition could be directly visualized. Again, I compared untransfected HEK293 cells with our stable HEK293-VMAT2 cell line. As an additional negative control, cells were incubated with buffer absent of FFN206, which did not cause any appreciable fluorescence (**Figure 23 A+C**). Then, both cell lines were incubated with FFN206-containing solutions (5 µM FFN206), leading to a strong signal in HEK293-VMAT2 cells (**Figure 23 F**) and to a comparatively weak signal in untransfected HEK293 cells (**Figure 23 B**), which corresponds to the background signal from unspecific binding/uptake of FFN206. Lastly, HEK293-VMAT2 cells were co-incubated with reserpine (4 µM) (**Figure 23 D**) or tetrabenazine (4 µM) (**Figure 23 E**) and FFN206: there still was some detectable signal but considerably weaker compared to FFN206 uptake without inhibitors (**Figure 23 F**). Lastly, **Figure 23 G** confirmed expression of VMAT2-eGFP in the stable HEK-VMAT2 line.

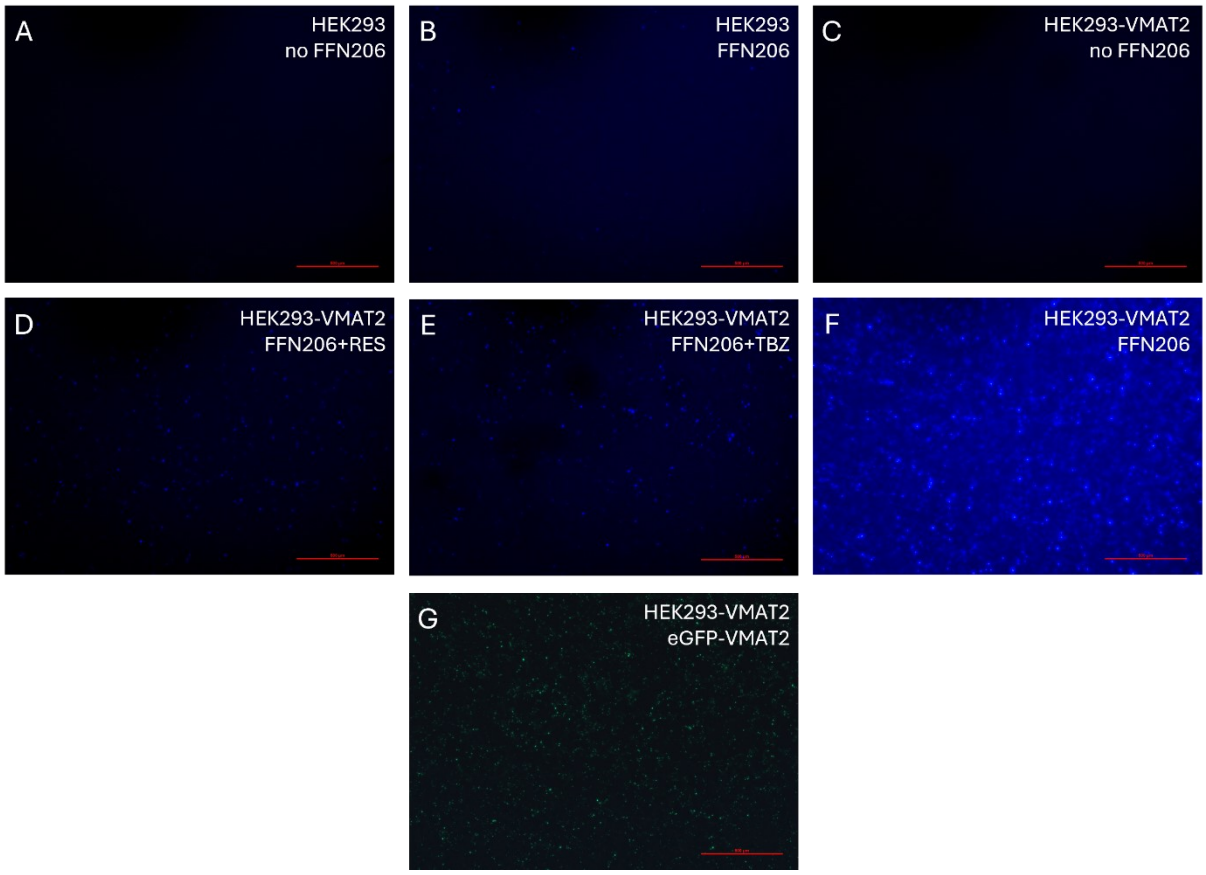

Figure 23: Fluorescent microscope images show FFN206 present in HEK293-VMAT2 cells after uptake, while in untransfected HEK293 cells there could no signal be detected. *As general negative control, first HEK293 cells were incubated with and without FFN206.* ***(A)*** *Incubation without FFN206 in untransfected HEK293 cells.* ***(B)*** *Incubation with FFN206 in untransfected HEK293 cells. Next, HEK293-VMAT2 cells were incubated with and without FFN206 as well as with FFN206 + reserpine/tetrabenazine.* ***(C)*** *Incubation without FFN206 (negative control) in HEK293-VMAT2 cells.* ***(D)*** *Incubation with FFN206 and reserpine in HEK293-VMAT2 cells.* ***(E)*** *Incubation with FFN206 and tetrabenazine in HEK293-VMAT2 cells.* ***(F)*** *Incubation with FFN206 (positive control) in HEK293-VMAT2 cells.* ***(G)*** *GFP channel depicting positions of VMAT2 transporters. FFN206 concentration was 5 µM, pre-incubation time was 30 min and incubation with FFN206 was 60 min at 37°C. All images were taken at 4x magnification, the drawn bars indicate 500 µm.*

After the initial tests, another FFN206 uptake assay was performed to determine dose-response relationships of FFN206 uptake with increasing concentrations of VMAT2 inhibitors (**Figure 24**). The fluorescence measured was reduced with increasing concentrations of inhibitor (**Figures 24+25**).

However, similar to the first uptakes, the difference between control (no inhibitor) and the condition without FFN206 was only about 6,000 RFU (**Figure 25 A+B**). Taken aside the outliers, overall the error bars indicated relatively high variability between replicates and again it has to be considered that the actual measured signal went up to around 45,000 RFU (**Figure 24**) compared to a maximum signal of about 7,000 RFU after baseline correction (**Figure 25 A+B**). That means that as it is, the FFN206 assay is not very sensitive, especially for small changes in signal intensities e.g. when measuring weaker effects like GABA inhibition. There seemed to be a dose-response to some extent (**Figure 25 C+D+E+F**), although the measured IC_{50} of approximately 6 µM (**Figure 25 E**) or 0.6 µM (**Figure 25 F**) were higher than expected (in the range of 10-110 nM) (Pidathala et al. 2023). Additionally, variable cell numbers per well possibly influenced the variability of these measurements. Accordingly, more testing and optimisation of this assay is warranted.

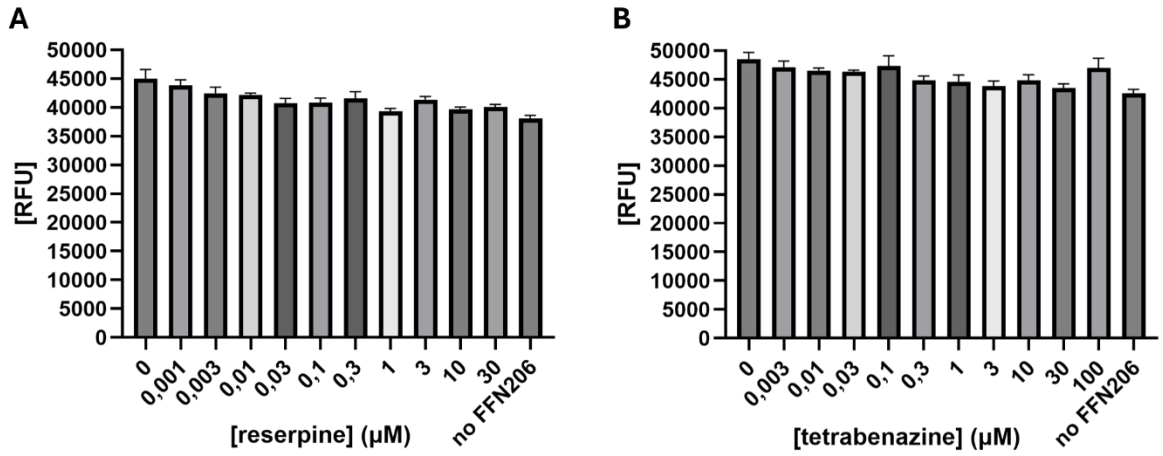

Figure 24: FFN206 uptake in HEK293-VMAT2 cells decreased with increasing concentrations of the VMAT2 antagonists reserpine or tetrabenazine. *Uptake of FFN206 was measured at 8 mm distance from the bottom of the wells, with different concentrations of reserpine **(A)** or tetrabenazine **(B)**. FFN206 concentration was 1 µM, pre-incubation time was 30 min and incubation with FFN206 was 60 min at 37°C.*

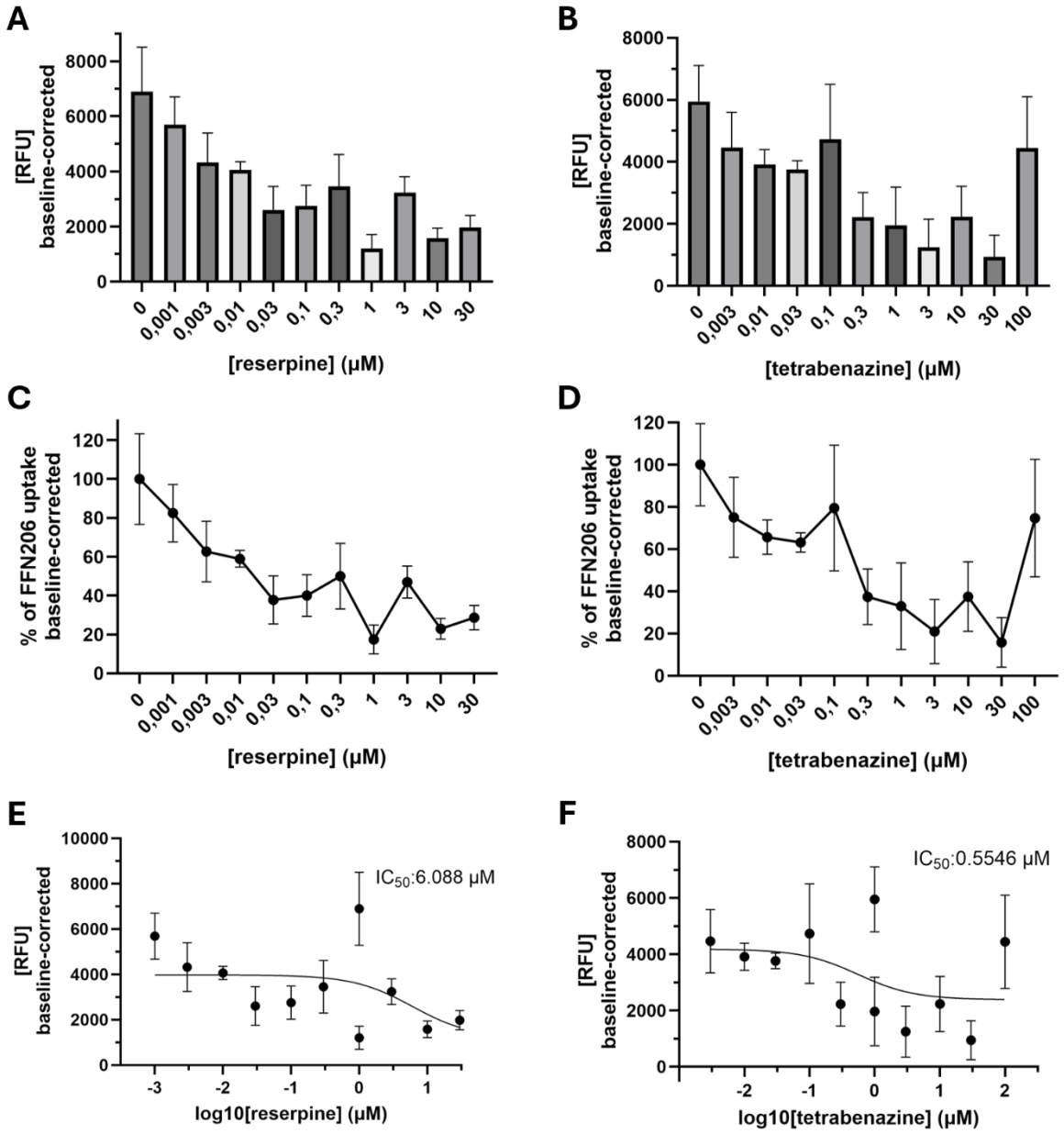

Figure 25: Baseline-corrected FFN206 uptake in HEK293-VMAT2 cells decreased with increasing concentrations of the VMAT2 antagonists reserpine or tetrabenazine. *Uptake of FFN206 was measured at 8 mm distance from the bottom of the wells. Results are shown after subtraction of the baseline (no FFN206) as RFU with different concentrations of reserpine* ***(A)*** *or tetrabenazine* ***(B)*** *and as % of FFN206 uptake with different concentrations of reserpine* ***(C)*** *or tetrabenazine* ***(D)****. Non-linear regression yielded an* IC_{50} *of ~6 µM for reserpine* ***(E)*** *and ~0.6 µM for tetrabenazine* ***(F)****. FFN206 concentration was 1 µM, pre-incubation time was 30 min and incubation with FFN206 was 60 min at 37°C.*

4.4 Co-immunoprecipitation and immunoblotting

In order to determine whether GAT1 and VMAT2 can co-precipitate from brain lysates, I started to also perform co-immunoprecipitation experiments. The idea was that if the two transporters are in close proximity, they should co-purify. If true, it may hint towards a mechanism making GABA uptake via VMAT2 possible due to local shunting, despite the rather low affinity of GABA at VMAT2.

For co-precipitation experiments, brain tissue or transfected cells with tagged transporters, i.e. YFP-GAT1 or YFP-VMAT2 (transient transfection) or GFP-VMAT2 (stable transfection), were lysed and incubated first with primary antibodies (anti-GAT1/VMAT2/GFP), then with protein G beads that bind the Fc regions of the primary antibodies (Akerström et al. 1985). In case of an interaction, tightly bound proteins should co-precipitate. I hypothesize that GAT1 interacts with VMAT2 and can therefore be pulled-down with an anti-VMAT2 antibody, and vice versa.

First, it was tested whether the antibodies against GAT1, VMAT2 or GFP would be specific for their designated epitopes. Therefore, the antibodies were first tested in different cell lines (either stably expressing HEK293-VMAT2 or transiently transfected Neuro2A (N2a) GAT1/GAT1+VMAT2 cells) and brain tissue (mouse striatum). Also, anti-VMAT2, anti-GFP and anti-GAT1 antibodies were tested for their applicability in co-immunoprecipitation (co-IP) experiments with the mouse striatum lysates.

Rat GAT1 has a molecular weight of approximately 67 kD (Guastella et al. 1990), while human GAT1 is expected around 70 kD (Zhu et al. 2023). Glycosylated GAT1 should show bands at 96 kD and 108 kD (Cai et al. 2005). For VMAT2, the predicted molecular weight is around 55 kD, while also a glycosylated form around 75 kD was reported (Jassen et al. 2005). Usually there are differentially glycosylated forms of transporters, that get N-glycosylated during synthesis and transport to their final destination (e.g. vesicle or plasma membrane). The N-glycosylation may affect protein stability and depending on the size, will result in a higher apparent molecular weight of the transporter (Ramamoorthy et al. 1998). I predict that in contrast to the endogenous forms, in my transfected cell lysates there are bands to be expected at around 95 kD or 125 kD (YFP-GAT1) and 80 kD or 100 kD (YFP/GFP-VMAT2). This is because the transporters for transient transfection are tagged with YFP which adds another 27 kD to the total molecular weight (Nishiuchi et al. 1998).

In the beginning, it was tested whether the primary antibodies are suitable for immunoblot detection, starting with the antibody against GAT1. In the first immunoblot (**Figure 26 A**), it seems like GAT1 detection with the rabbit anti-GAT1 primary antibody was successful for mouse brain lysates. This is because the band at 70 kD was getting fainter with higher incubation temperature while at the top there was a band slightly getting stronger, which looks like it is due to aggregation of GAT1. It is also noteworthy that there seem to be unspecific bands around 55 kD with high intensity throughout all samples. In **Figure 26 B**, the results were less clear. While in the HEK-VMAT2 sample the bands around 70 kD (GAT1) and 100 kD (glycosylated GAT1) could be from GAT1, the N2a-GAT1 sample showed only one intense band at around 115 kD and the STR sample at 55 kD. The latter looks similar to the presumably unspecific bands from mouse brain samples (**Figure 26 A**), while the 115 kD band from the N2a-GAT1 sample represented a glycosylated form of GAT1 at best. In the last immunoblot (**Figure 26 C**), additionally two different incubation temperatures were tested, namely 95 °C for 3 min and 50 °C for 15 min. A band from GAT1 would be expected to decrease in intensity with increasing heat because of GAT1 aggregation, which was only true for the band around 125 kD. This either means that said band came from a glycosylated form of GAT1 or that there were no specific bands. Furthermore, similar to the probably unspecific bands around 55 kD in mouse brain samples (**Figure 26 A+B**), in the N2a-GAT1 samples (**Figure 26 C**) there seemed to be unspecific bands around 36 kD.

Overall, these results indicate that the rabbit anti-GAT1 antibody did work for GAT1 immunoblot detection from mouse brain samples, but not so well with cell lysates. Additionally, there might be a specificity problem, looking at mentioned unspecific bands.

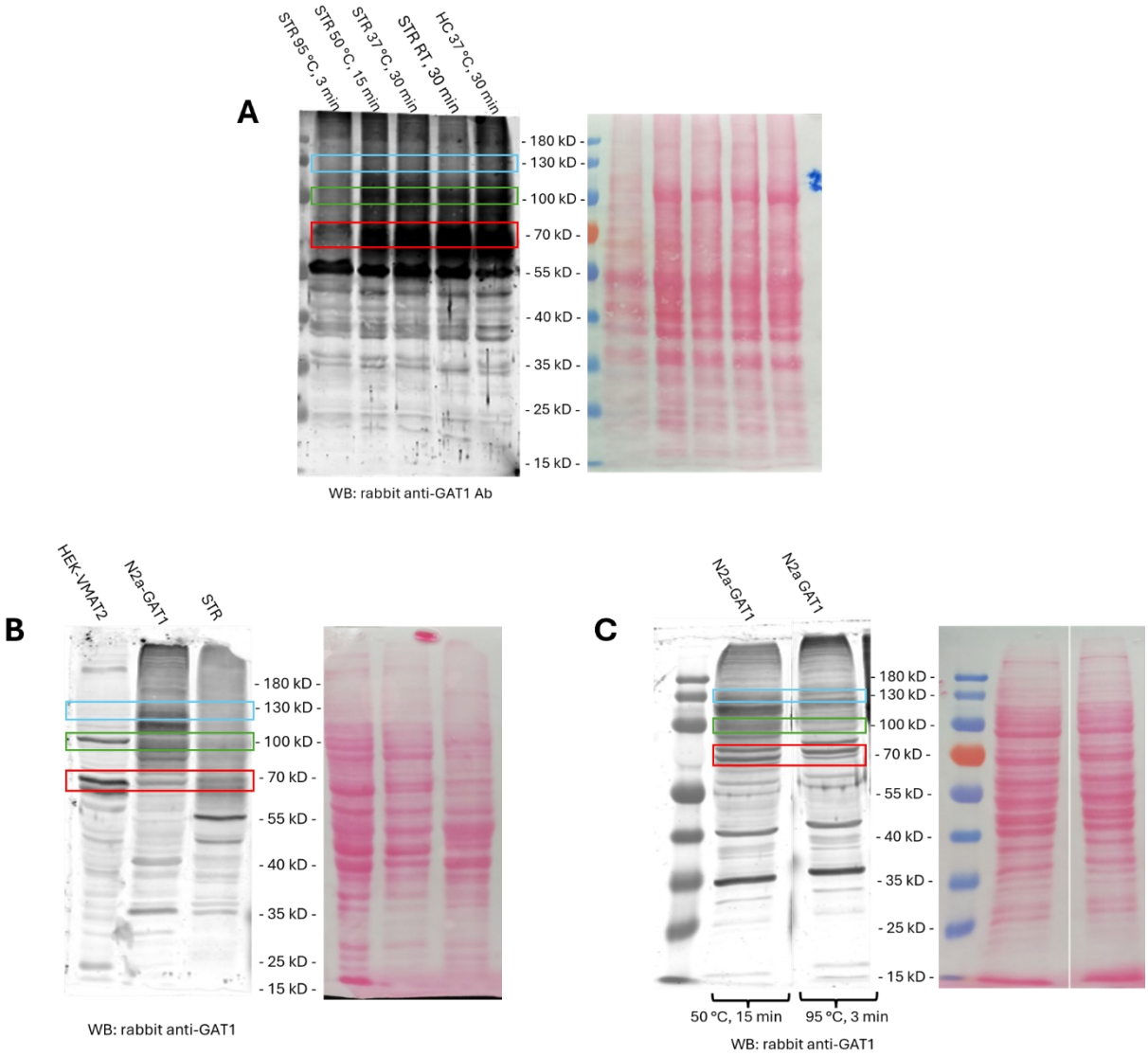

Figure 26: GAT1 detection using a rabbit anti-GAT1 antibody did presumably work for immunoblot detection. ***(A)*** *Western blots (WBs) of mouse striatum (STR) or hippocampus (HC) lysates are shown. Incubation before loading on the gel for SDS-PAGE was done at 95 °C for 3 min, 50 °C for 15 min and 37 °C or room temperature (RT) for 30 min.* ***(B)*** *WBs of stably transfected HEK293-VMAT2 (HEK-VMAT2) cells, transiently YFP-GAT1-transfected N2a (N2a-GAT1) cells and mouse striatum lysates (STR) are shown. Incubation before loading on the gel for SDS-PAGE was done at 50 °C for 15 min.* ***(C)*** *WBs of transiently YFP-GAT1-transfected N2a (N2a-GAT1) cell lysates are shown. Incubation before loading on the gel for SDS-PAGE was either done at 95 °C for 3 min or at 50 °C for 15 min. Primary antibodies for the WBs were rabbit anti-GAT1 (1:2000 for* ***(B)*** *or 1:1000 for* ***(A)*** *and* ***(C)****), secondary antibody was goat anti-rabbit (1:5000). Shown on the right side of each blot is a Ponceau S staining of the blotting membrane. Coloured frames indicate where bands would be expected: endogenous unmodified GAT1* ***(red)****, YFP-GAT1 or endogenous glycosylated GAT1* ***(green)****, glycosylated YFP-GAT1* ***(blue)***

The next immunoblots I performed to do a similar test like before with primary antibodies directed either against VMAT2 directly or against the GFP/YFP-tag. Both immunoblots (**Figure 27 A+B**) did not show bands with high intensities, only some faint ones around 65 kD, 90 kD and 100 kD (**Figure 27 B**). As mentioned in this chapter, GFP/YFP-tagged VMAT2 is expected to produce bands around 80 kD or at 100 kD in its glycosylated form. Bands could be seen with approximately these molecular weights (**Figure 27 B, green and blue frames**), but given the low intensity and that the bands looked the same in untransfected HEK293 cells, they were not likely to reliably indicate VMAT2 detection; since in untransfected cells there is no tagged VMAT2 present, there should not be any band detected with an anti-GFP antibody.

Taken together, these results indicated that neither the rabbit anti-VMAT2 antibody nor the mouse anti-GFP antibody are well suited for tagged VMAT2 detection in immunoblots. At least in the HEK-VMAT2, HEK-VM2-GAT1 and mouse striatum samples, there should be clearly visible VMAT2 bands. Judging from the Ponceau S staining (**Figure 27 A+B**) there were proteins of the expected size on the membranes, but presumably either the sensitivity was not high enough for detection with the antibodies or the antibodies were not specific.

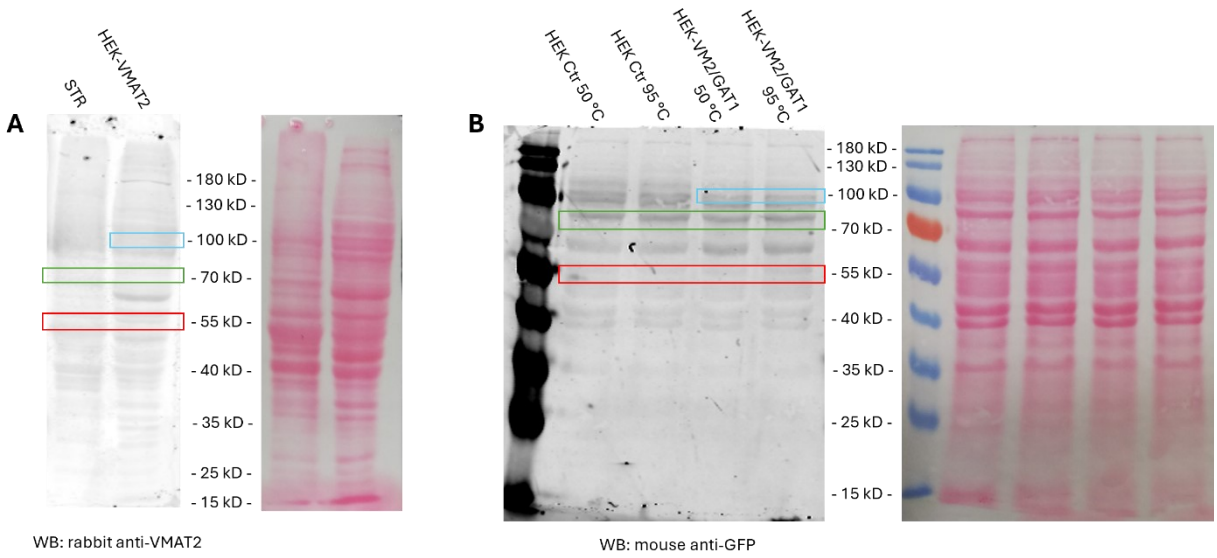

Figure 27*: VMAT2 detection using a rabbit anti-GAT1 or a mouse anti-GFP antibody did not work for immunoblot detection. *(A) *Western blots (WBs) of stably transfected HEK293-VMAT2 cells (HEK-VMAT2) and mouse striatum (STR) lysates are shown. Incubation before loading on the gel for SDS-PAGE was done at 50 °C for 15 min.* ***(B)*** *Shown are WBs of lysates from untransfected HEK293 cells (HEK Ctr) and HEK293 cells that were transiently transfected with both GAT1 and YFP-VMAT2 (HEK-VM2/GAT1). Incubation before loading on the gel for SDS-PAGE was either done 95 °C for 3 min or at 50 °C for 15 min Primary antibodies for the WBs were rabbit anti-VMAT2 (1:2000)* ***(A)*** *or mouse anti-GFP (1:1000)* ***(B)****, secondary antibodies were goat anti-rabbit (1:5000)* ***(A)*** *or goat anti-mouse (1:5000)* ***(B)****. Shown on the right side of each blot is a Ponceau S staining of the blotting membrane. Coloured frames indicate where bands would be expected: endogenous unmodified VMAT2* ***(red)****, YFP/GFP-VMAT2 or endogenous glycosylated VMAT2* ***(green)****, glycosylated YFP-VMAT2* ***(blue)***

Finally, I started to perform co-immunoprecipitation (co-IP) experiments to test whether the primary antibodies are suitable for these experiments. Co-IPs were done from N2a cells transiently transfected with YFP-GAT1 (**Figure 28 A**), mouse striatum lysates (**Figure 28 B**) and with HEK293 cells transiently transfected with GAT1 and YFP-VMAT2 (**Figure 28 C**)

What one can see immediately when looking at the immunoblots (**Figure 28**), is that although loading the same overall amount of protein as in the previous blots (**Figures 26 + 27**), there were almost no proteins visible in the Ponceau S staining. This could mean that the co-IP of GAT1 and VMAT2 was successful, since only proteins interacting with GAT1 or VMAT2 should theoretically be enriched in that process. Most likely though, the stronger bands at 23 kD, 50 kD and 73 kD correspond to the light, heavy or light + heavy chains of the primary antibody (IgG) used for pulldown (Björk and Tanford 1971). The 73 kD band is only expected from intact whole IgG (Björk and Tanford 1971) and indicates inadequate reduction of disulfide bonds between heavy and light chains of the antibody during sample preparation (Hagihara and Saerens 2014). Overall, the blot looked rather unspecific because the bands are mainly in the range of IgG heavy, light or heavy + light chains. For instance, there are bands around 70 kD (**Figure 28, A+B+C**) and 50 kD (**Figure 28, A+B+C**) that could resemble GAT1 or VMAT2, but might as well be from IgG.

From these preliminary results it was concluded that the co-IP of GAT1 and VMAT2 likely did not work, but that there was also possibly some problem with the antibody specificity leading to detection of no bands (anti-VMAT2) or unspecific bands (anti-GAT1), e.g. at 55 kD in all mouse brain samples. The main problem might be that the used primary antibodies for co-IP and immunoblot in most cases were from the same species. One solution against IgG bands therefore could be to use different primary antibodies for co-IP and immunoblot (i.e. different species). For instance, when examining the transfected cell lysates, one could use a primary mouse anti-GFP antibody for either the co-IP or the immunoblot detection and a rabbit anti-GAT1 antibody for the other one (like in **Figure 28 C**), since the transporters are YFP-tagged. This might have yielded better results than using rabbit anti-GAT1 for co-IP as well as immunoblot detection, although this is unclear when looking at **Figure 28 C**; for instance there still are presumably unspecific bands around 35 kD, as it already was in **Figure 26 C** for the cell lysates. The immunoblots in **Figure 28 A+B** did not yield clear results, since almost all lanes looked similar to each other. Only from **Figure 28 C** one could guess that maybe co-IP and immunoblot worked with the antibodies. This is because for the co-IPs with both anti-VMAT2 and anti-GAT1 there were bands getting fainter around 100 kD, which would be in the range of either glycosylated GAT1 or glycosylated YFP-VMAT2.

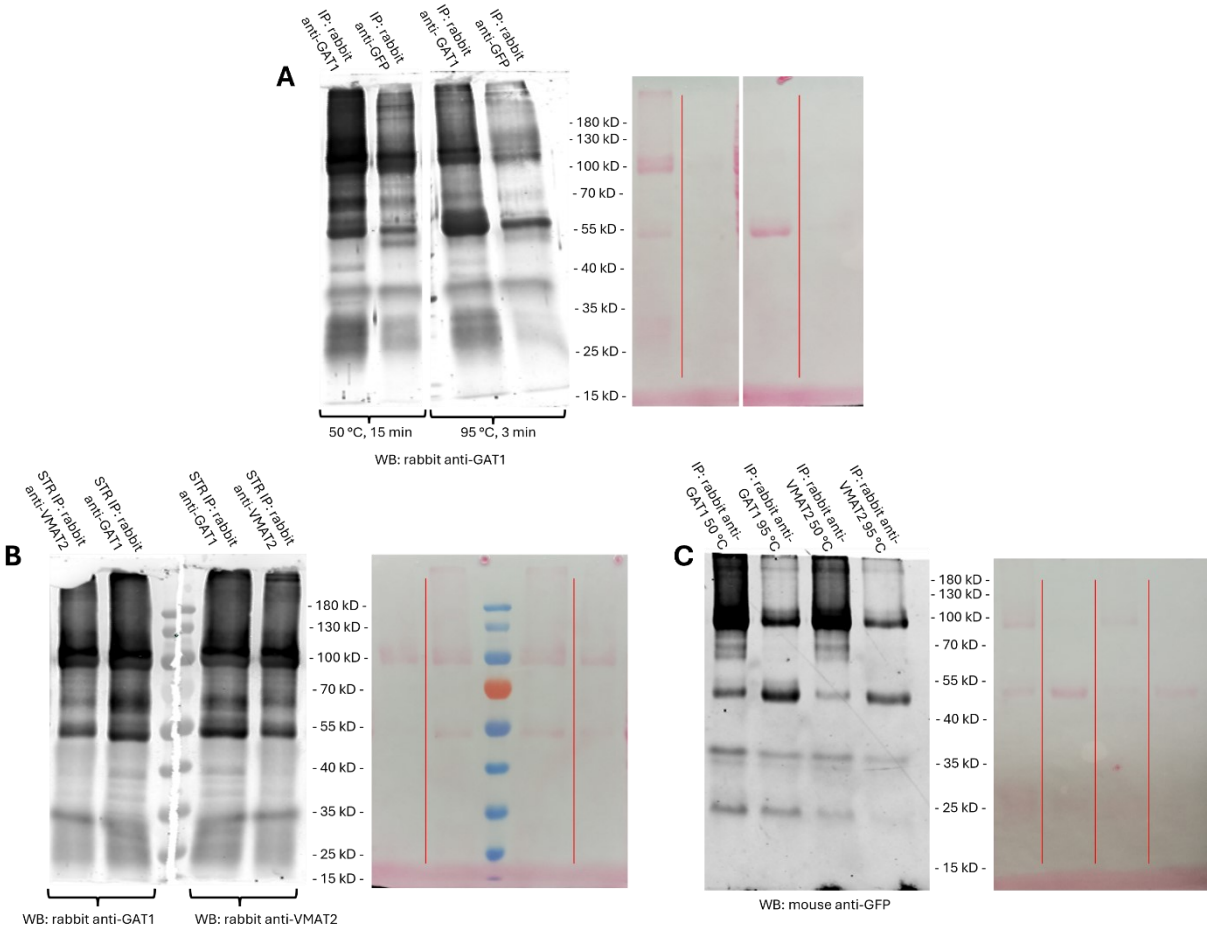

***Figure 28*: Co-immunoprecipitation of VMAT2 and GAT1 presumably did not work. (A)** *Shown is a western blot (WB) of co-immunoprecipitations (co-IPs) with antibodies against GAT1 and GFP from lysates of transiently YFP-GAT1-transfected N2a cells. Incubation before loading on the gel for SDS-PAGE was either done at 95 °C for 3 min or at 50 °C for 15 min.* **(B)** *Shown is a WB of co-IPs with antibodies against GAT1 and VMAT2 from mouse striatum lysates. Incubation before loading on the gel for SDS-PAGE was done at 50 °C for 15 min.* **(C)** *Shown is a WB of co-IPs with antibodies against GAT1 and VMAT2 from HEK293 cells that were transiently transfected with YFP-VMAT2 and GAT1. Incubation before loading on the gel for SDS-PAGE was done at 50 °C for 15 min. Primary antibodies for the WBs were rabbit anti-GAT1 at 1:1000* **(A)** *or 1:2000* **(B)**, *rabbit anti-VMAT2 (1:2000)* **(B)** *and mouse anti-GFP (1:1000)* **(C)**, *secondary antibody was goat anti-rabbit (1:5000)* **(A)**+**(B)** *and goat anti-mouse (1:5000)* **(C)**. *Shown on the right side of each blot is a Ponceau S staining of the blotting membrane. Red vertical lines indicate separate lanes.*

5 Summary and outlook

Radiotracer flux measurements (using [^{3}H]5-HT and [^{3}H]GABA) as well as radioligand binding assays (using [^{3}H]DTBZ) were conducted in striatal or cerebellar synaptic vesicles, doing inhibition curves with unlabelled GABA, glycine or taurine. From the [^{3}H]5-HT uptakes it was concluded that GABA decreased [^{3}H]5-HT uptake at high millimolar concentrations, while glycine overall did not reduce uptake at all and taurine had a similar effect to GABA. This could mean that GABA is a weak VMAT2 substrate; similarly, taurine could be a weak VMAT2 substrate and as a possible $GABA_A$ receptor ligand might have induced oIPSCs in the experiments of Tritsch et al., while glycine does not seem to play an important role here.

More experiments in human synaptic vesicles would be desirable, since we were short on tissue and as discussed, most of the samples cannot be used for uptake assays in the first place. The most interesting experiment would have been direct [^{3}H]GABA uptake into striatal synaptic vesicles, but unfortunately the results cannot be used because even the controls did not yield clear results. What could help for future experiments would be to use more concentrated and/or better purified synaptic vesicle preparations in larger volumes, as well as higher amounts of [^{3}H]GABA per sample; both is not that easy because of limited availability or high expenses. In the binding experiments, GABA was not able to displace [^{3}H]DTBZ which was almost to be expected, since TBZ is a high-affinity ligand of VMAT2 while GABA presumably has a weak affinity.

The FFN206 experiments indicated that FFN206 may be a suitable substrate for future VMAT2 studies in the lab. Because of limited time, the FFN206 experiments could not be further pursued and refined.

Co-immunoprecipitation experiments with immunoblots were performed to test the antibodies for that application and to find out, whether there might be an interaction between GAT1 and VMAT2, yielding unclear results for now. For future experiments, maybe different antibodies should be used (with different species for the co-immunoprecipitation and the immunoblots), also to better distinguish between bands from the transporters and bands from the IgG. What could then be tried additionally is to incubate with a crosslinker before lysing the cells/tissue for co-immunoprecipitation, to see if there are differences in pulling down GAT1 and VMAT2 together.

Generally, the next steps besides optimising the utilised protocols would be *in vivo* experiments in mice, trying to further deepen the understanding of how GABA co-release from midbrain DA neurons works and then also what the physiological role might be, e.g. in Parkinson's Disease.

6 Literature

Akerström, B, T Brodin, K Reis, and L Björck. 1985. 'Protein G: A Powerful Tool for Binding and Detection of Monoclonal and Polyclonal Antibodies.' *The Journal of Immunology* 135 (4): 2589–92. https://doi.org/10.4049/jimmunol.135.4.2589.

Alvarez, Adrian, José M. Costa-Fernández, Rosario Pereiro, Alfredo Sanz-Medel, and Alfonso Salinas-Castillo. 2011. 'Fluorescent Conjugated Polymers for Chemical and Biochemical Sensing'. *TrAC Trends in Analytical Chemistry* 30 (9): 1513–25. https://doi.org/10.1016/j.trac.2011.04.017.

Armstrong, J., and R.B. Barlow. 1976. 'THE IONIZATION OF PHENOLIC AMINES, INCLUDING APOMORPHINE, DOPAMINE AND CATECHOLAMINES AND AN ASSESSMENT OF ZWITTERION CONSTANTS'. *British Journal of Pharmacology* 57 (4): 501–16. https://doi.org/10.1111/j.1476-5381.1976.tb10377.x.

Bissonette, G. B., and M. R. Roesch. 2016. 'Development and Function of the Midbrain Dopamine System: What We Know and What We Need To'. *Genes, Brain and Behavior* 15 (1): 62–73. https://doi.org/10.1111/gbb.12257.

Björk, Ingemar, and Charles Tanford. 1971. 'Recovery of Native Conformation of Rabbit Immunoglobulin G upon Recombination of Separately Renatured Heavy and Light Chains at Near-Neutral pH'. *Biochemistry* 10 (8): 1289–95. https://doi.org/10.1021/bi00784a003.

Björklund, Anders, and Stephen B. Dunnett. 2007. 'Dopamine Neuron Systems in the Brain: An Update'. *Trends in Neurosciences* 30 (5): 194–202. https://doi.org/10.1016/j.tins.2007.03.006.

Bowery, N G, and T G Smart. 2006. 'GABA and Glycine as Neurotransmitters: A Brief History'. *British Journal of Pharmacology* 147 (S1). https://doi.org/10.1038/sj.bjp.0706443.

Cai, Guoqiang, Petrus S. Salonikidis, Jian Fei, Wolfgang Schwarz, Ralf Schülein, Werner Reutter, and Hua Fan. 2005. 'The Role of N-glycosylation in the Stability, Trafficking and GABA-uptake of GABA-transporter 1: Terminal N-glycans Facilitate Efficient GABA-uptake Activity of the GABA Transporter'. *The FEBS Journal* 272 (7): 1625–38. https://doi.org/10.1111/j.1742-4658.2005.04595.x.

Chaudhry, Farrukh A., Richard J. Reimer, Elizabeth E. Bellocchio, Niels C. Danbolt, Kirsten K. Osen, Robert H. Edwards, and Jon Storm-Mathisen. 1998. 'The Vesicular GABA Transporter, VGAT, Localizes to Synaptic Vesicles in Sets of Glycinergic as Well as GABAergic Neurons'. *The Journal of Neuroscience* 18 (23): 9733–50. https://doi.org/10.1523/JNEUROSCI.18-23-09733.1998.

Chen, Nian-Hang, Maarten E. A. Reith, and Michael W. Quick. 2004. 'Synaptic Uptake and beyond: The Sodium- and Chloride-Dependent Neurotransmitter Transporter Family SLC6'. *Pflügers Archiv European Journal of Physiology* 447 (5): 519–31. https://doi.org/10.1007/s00424-003-1064-5.

Choi, Dennis W. 1992. 'Excitotoxic Cell Death'. *Journal of Neurobiology* 23 (9): 1261–76. https://doi.org/10.1002/neu.480230915.

Cidon, S, and T S Sihra. 1989. 'Characterization of a H+-ATPase in Rat Brain Synaptic Vesicles'. *Journal of Biological Chemistry* 264 (14): 8281–88. https://doi.org/10.1016/s0021-9258(18)83180-5.

Dalton, Michael P, Mary Hongying Cheng, Ivet Bahar, and Jonathan A Coleman. 2024. 'Structural Mechanisms for VMAT2 Inhibition by Tetrabenazine'. *eLife* 12 (March):RP91973. https://doi.org/10.7554/eLife.91973.

Edwards, Robert H. 2007. 'The Neurotransmitter Cycle and Quantal Size'. *Neuron* 55 (6): 835–58. https://doi.org/10.1016/j.neuron.2007.09.001.

Eskenazi, Daniel, Lauren Malave, Susana Mingote, Leora Yetnikoff, Samira Ztaou, Vlad Velicu, Stephen Rayport, and Nao Chuhma. 2021. 'Dopamine Neurons That Cotransmit Glutamate, From Synapses to Circuits to Behavior'. *Frontiers in Neural Circuits* 15 (May):665386. https://doi.org/10.3389/fncir.2021.665386.

Featherstone, David E. 2010. 'Intercellular Glutamate Signaling in the Nervous System and Beyond'. *ACS Chemical Neuroscience* 1 (1): 4–12. https://doi.org/10.1021/cn900006n.

Finn, J. Patrick, and Robert H. Edwards. 1997. 'Individual Residues Contribute to Multiple Differences in Ligand Recognition between Vesicular Monoamine Transporters 1 and 2'. *Journal of Biological Chemistry* 272 (26): 16301–7. https://doi.org/10.1074/jbc.272.26.16301.

Fon, Edward A., and Robert H. Edwards. 2001. 'Molecular Mechanisms of Neurotransmitter Release'. *Muscle & Nerve* 24 (5): 581–601. https://doi.org/10.1002/mus.1044.

Fonnum, Frode. 1984. 'Glutamate: A Neurotransmitter in Mammalian Brain'. *Journal of Neurochemistry* 42 (1): 1–11. https://doi.org/10.1111/j.1471-4159.1984.tb09689.x.

Fuxe, Kjell, Annica B. Dahlström, Gösta Jonsson, Daniel Marcellino, Michele Guescini, Mauro Dam, Paul Manger, and Luigi Agnati. 2010. 'The Discovery of Central Monoamine Neurons Gave Volume Transmission to the Wired Brain'. *Progress in Neurobiology* 90 (2): 82–100. https://doi.org/10.1016/j.pneurobio.2009.10.012.

Guastella, John, Nathan Nelson, Hannah Nelson, Linda Czyzyk, Shoshi Keynan, May C. Miedel, Norman Davidson, Henry A. Lester, and Baruch I. Kanner. 1990. 'Cloning and Expression of a Rat Brain GABA Transporter'. *Science* 249 (4974): 1303–6. https://doi.org/10.1126/science.1975955.

Gubernator, Niko G., Hui Zhang, Roland G. W. Staal, Eugene V. Mosharov, Daniela B. Pereira, Minerva Yue, Vojtech Balsanek, et al. 2009. 'Fluorescent False Neurotransmitters Visualize Dopamine Release from Individual Presynaptic

Terminals'. *Science* 324 (5933): 1441–44. https://doi.org/10.1126/science.1172278.

Hagihara, Yoshihisa, and Dirk Saerens. 2014. 'Engineering Disulfide Bonds within an Antibody'. *Biochimica et Biophysica Acta (BBA) - Proteins and Proteomics* 1844 (11): 2016–23. https://doi.org/10.1016/j.bbapap.2014.07.005.

Hertz, Leif, Ralf Dringen, Arne Schousboe, and Stephen R. Robinson. 1999. 'Astrocytes: Glutamate Producers for Neurons'. *Journal of Neuroscience Research* 57 (4): 417–28. https://doi.org/10.1002/(SICI)1097-4547(19990815)57:4<417::AID-JNR1>3.0.CO;2-N.

Hnasko, Thomas S., Nao Chuhma, Hui Zhang, Germaine Y. Goh, David Sulzer, Richard D. Palmiter, Stephen Rayport, and Robert H. Edwards. 2010. 'Vesicular Glutamate Transport Promotes Dopamine Storage and Glutamate Corelease In Vivo'. *Neuron* 65 (5): 643–56. https://doi.org/10.1016/j.neuron.2010.02.012.

Hu, Gang, Adam Henke, Richard J. Karpowicz, Mark S. Sonders, Frances Farrimond, Robert Edwards, David Sulzer, and Dalibor Sames. 2013. 'New Fluorescent Substrate Enables Quantitative and High-Throughput Examination of Vesicular Monoamine Transporter 2 (VMAT2)'. *ACS Chemical Biology* 8 (9): 1947–54. https://doi.org/10.1021/cb400259n.

Ilic, Marija, Julian Maier, Marion Holy, Kathrin Jaentsch, Matthias E. Liechti, Gert Lubec, Michael H. Baumann, Harald H. Sitte, and Dino Luethi. 2020. 'Cell-Based Radiotracer Binding and Uptake Inhibition Assays: A Comparison of In Vitro Methods to Assess the Potency of Drugs That Target Monoamine Transporters'. *Frontiers in Pharmacology* 11 (May):673. https://doi.org/10.3389/fphar.2020.00673.

Jassen, Amy K., Jeffrey M. Brown, Helen N. Panas, Gregory M. Miller, Danqing Xiao, and Bertha K. Madras. 2005. 'Variants of the Primate Vesicular Monoamine Transporter-2'. *Molecular Brain Research* 139 (2): 251–57. https://doi.org/10.1016/j.molbrainres.2005.05.028.

Johnson, R.G., S.E. Carty, and A. Scarpa. 1981. 'Proton: Substrate Stoichiometries during Active Transport of Biogenic Amines in Chromaffin Ghosts.' *Journal of Biological Chemistry* 256 (11): 5773–80. https://doi.org/10.1016/s0021-9258(19)69274-4.

Jonas, Peter, Josef Bischofberger, and Jürgen Sandkühler. 1998. 'Corelease of Two Fast Neurotransmitters at a Central Synapse'. *Science* 281 (5375): 419–24. https://doi.org/10.1126/science.281.5375.419.

Kim, Jae-Ick, Subhashree Ganesan, Sarah X. Luo, Yu-Wei Wu, Esther Park, Eric J. Huang, Lu Chen, and Jun B. Ding. 2015. 'Aldehyde Dehydrogenase 1a1 Mediates a GABA Synthesis Pathway in Midbrain Dopaminergic Neurons'. *Science* 350 (6256): 102–6. https://doi.org/10.1126/science.aac4690.

Knoth, Jane, Michael Zallakian, and David Njus. 1981. 'Stoichiometry of Hydrogen Ion-Linked Dopamine Transport in Chromaffin Granule Ghosts'. *Biochemistry* 20 (23): 6625–29. https://doi.org/10.1021/bi00526a016.

Krishek, B J, A Amato, C N Connolly, S J Moss, and T G Smart. 1996. 'Proton Sensitivity of the GABA(A) Receptor Is Associated with the Receptor Subunit Composition.' *The Journal of Physiology* 492 (2): 431–43. https://doi.org/10.1113/jphysiol.1996.sp021319.

Li, Shuxin, and Peter K. Stys. 2000. 'Mechanisms of Ionotropic Glutamate Receptor-Mediated Excitotoxicity in Isolated Spinal Cord White Matter'. *The Journal of Neuroscience* 20 (3): 1190–98. https://doi.org/10.1523/JNEUROSCI.20-03-01190.2000.

Limani, Fabian, Sivakumar Srinivasan, Michaela Hanzlova, Ségolène La Batide-Alanore, Sigrid Klotz, Thomas S. Hnaskoxs, and Thomas Steinkellner. 2024. 'Evidence for Low Affinity of GABA at the Vesicular Monoamine Transporter VMAT2 – Implications for Transmitter Co-Release from Dopamine Neurons'. https://doi.org/10.1101/2024.07.04.602053.

Lin, Lawrence, Sook Wah Yee, Richard B. Kim, and Kathleen M. Giacomini. 2015. 'SLC Transporters as Therapeutic Targets: Emerging Opportunities'. *Nature Reviews Drug Discovery* 14 (8): 543–60. https://doi.org/10.1038/nrd4626.

Maycox, P R, T Deckwerth, J W Hell, and R Jahn. 1988. 'Glutamate Uptake by Brain Synaptic Vesicles. Energy Dependence of Transport and Functional Reconstitution in Proteoliposomes.' *Journal of Biological Chemistry* 263 (30): 15423–28. https://doi.org/10.1016/s0021-9258(19)37605-7.

McIntire, Steven L., Richard J. Reimer, Kim Schuske, Robert H. Edwards, and Erik M. Jorgensen. 1997. 'Identification and Characterization of the Vesicular GABA Transporter'. *Nature* 389 (6653): 870–76. https://doi.org/10.1038/39908.

Meera, Pratap, Mikko Uusi-Oukari, Gerald S. Lipshutz, and Martin Wallner. 2023. 'GABAA Receptors as Plausible Molecular Targets and Mediators for Taurine and Homotaurine Actions'. *Frontiers in Pharmacology* 14 (December):1271203. https://doi.org/10.3389/fphar.2023.1271203.

Melani, Riccardo, and Nicolas X. Tritsch. 2022. 'Inhibitory Co-Transmission from Midbrain Dopamine Neurons Relies on Presynaptic GABA Uptake'. *Cell Reports* 39 (3): 110716. https://doi.org/10.1016/j.celrep.2022.110716.

Nelson, E.L., C.-L. Liang, C.M. Sinton, and D.C. German. 1996. 'Midbrain Dopaminergic Neurons in the Mouse: Computer-Assisted Mapping'. *The Journal of Comparative Neurology* 369 (3): 361–71. https://doi.org/10.1002/(SICI)1096-9861(19960603)369:3<361::AID-CNE3>3.0.CO;2-3.

Niciu, Mark J., Benjamin Kelmendi, and Gerard Sanacora. 2012. 'Overview of Glutamatergic Neurotransmission in the Nervous System'. *Pharmacology*

Biochemistry and Behavior 100 (4): 656–64. https://doi.org/10.1016/j.pbb.2011.08.008.

Nishiuchi, Yuji, Tatsuya Inui, Hideki Nishio, József Bódi, Terutoshi Kimura, Frederick I. Tsuji, and Shumpei Sakakibara. 1998. 'Chemical Synthesis of the Precursor Molecule of the *Aequorea* Green Fluorescent Protein, Subsequent Folding, and Development of Fluorescence'. *Proceedings of the National Academy of Sciences* 95 (23): 13549–54. https://doi.org/10.1073/pnas.95.23.13549.

Patterson, George, Rich N. Day, and David Piston. 2001. 'Fluorescent Protein Spectra'. *Journal of Cell Science* 114 (5): 837–38. https://doi.org/10.1242/jcs.114.5.837.

Pidathala, Shabareesh, Shuyun Liao, Yaxin Dai, Xiao Li, Changkun Long, Chi-Lun Chang, Zhe Zhang, and Chia-Hsueh Lee. 2023. 'Mechanisms of Neurotransmitter Transport and Drug Inhibition in Human VMAT2'. *Nature* 623 (7989): 1086–92. https://doi.org/10.1038/s41586-023-06727-9.

Pifl, C., A. Rajput, H. Reither, J. Blesa, C. Cavada, J. A. Obeso, A. H. Rajput, and O. Hornykiewicz. 2014. 'Is Parkinson's Disease a Vesicular Dopamine Storage Disorder? Evidence from a Study in Isolated Synaptic Vesicles of Human and Nonhuman Primate Striatum'. *Journal of Neuroscience* 34 (24): 8210–18. https://doi.org/10.1523/JNEUROSCI.5456-13.2014.

Pifl, Christian, Harald Reither, Johannes Attems, and Luigi Zecca. 2023. 'Dopamine and Vesicular Monoamine Transport Loss Supports Incidental Lewy Body Disease as Preclinical Idiopathic Parkinson'. *Npj Parkinson's Disease* 9 (1): 89. https://doi.org/10.1038/s41531-023-00514-z.

Pratuangdejkul, Jaturong, Wichit Nosoongnoen, Georges-Alexandre Guérin, Sylvan Loric, Marc Conti, Jean-Marie Launay, and Philippe Manivet. 2006. 'Conformational Dependence of Serotonin Theoretical pKa Prediction'. *Chemical Physics Letters* 420 (4–6): 538–44. https://doi.org/10.1016/j.cplett.2006.01.035.

Ramamoorthy, Sammanda, Haley E. Melikian, Yan Qian, and Randy D. Blakely. 1998. '[24] Biosynthesis, N-Glycosylation, and Surface Trafficking of Biogenic Amine Transporter Proteins'. In *Methods in Enzymology*, 296:347–70. Elsevier. https://doi.org/10.1016/S0076-6879(98)96026-8.

Ro, Hyun-ah, and John H. Carson. 2004. 'pH Microdomains in Oligodendrocytes'. *Journal of Biological Chemistry* 279 (35): 37115–23. https://doi.org/10.1074/jbc.M403099200.

Rodrigo, M.M., M.A. Esteso, M.F. Barros, L.M.P. Verissimo, C.M. Romero, A.F. Suarez, M.L. Ramos, A.J.M. Valente, H.D. Burrows, and A.C.F. Ribeiro. 2017. 'The Structure and Diffusion Behaviour of the Neurotransmitter γ-Aminobutyric Acid (GABA) in Neutral Aqueous Solutions'. *The Journal of Chemical Thermodynamics* 104 (January):110–17. https://doi.org/10.1016/j.jct.2016.09.014.

Stan, Ana D., Subroto Ghose, Xue-Min Gao, Rosalinda C. Roberts, Kelly Lewis-Amezcua, Kimmo J. Hatanpaa, and Carol A. Tamminga. 2006. 'Human Postmortem Tissue:

What Quality Markers Matter?' *Brain Research* 1123 (1): 1–11. https://doi.org/10.1016/j.brainres.2006.09.025.

Steinkellner, Thomas, William S Conrad, Imre Kovacs, Robert A Rissman, Edward B Lee, John Q Trojanowski, Zachary Freyberg, et al. 2022. 'Dopamine Neurons Exhibit Emergent Glutamatergic Identity in Parkinson's Disease'. *Brain* 145 (3): 879–86. https://doi.org/10.1093/brain/awab373.

Steinkellner, Thomas, Vivien Zell, Zachary J. Farino, Mark S. Sonders, Michael Villeneuve, Robin J. Freyberg, Serge Przedborski, Wei Lu, Zachary Freyberg, and Thomas S. Hnasko. 2018. 'Role for VGLUT2 in Selective Vulnerability of Midbrain Dopamine Neurons'. *Journal of Clinical Investigation* 128 (2): 774–88. https://doi.org/10.1172/JCI95795.

Strata, Piergiorgio, and Robin Harvey. 1999. 'Dale's Principle'. *Brain Research Bulletin* 50 (5–6): 349–50. https://doi.org/10.1016/S0361-9230(99)00100-8.

Takamori, Shigeo. 2006. 'VGLUTs: "Exciting" Times for Glutamatergic Research?' *Neuroscience Research* 55 (4): 343–51. https://doi.org/10.1016/j.neures.2006.04.016.

Takamori, Shigeo, Dietmar Riedel, and Reinhard Jahn. 2000. 'Immunoisolation of GABA-Specific Synaptic Vesicles Defines a Functionally Distinct Subset of Synaptic Vesicles'. *The Journal of Neuroscience* 20 (13): 4904–11. https://doi.org/10.1523/JNEUROSCI.20-13-04904.2000.

Tritsch, Nicolas X., Jun B. Ding, and Bernardo L. Sabatini. 2012. 'Dopaminergic Neurons Inhibit Striatal Output through Non-Canonical Release of GABA'. *Nature* 490 (7419): 262–66. https://doi.org/10.1038/nature11466.

Tritsch, Nicolas X., Adam J. Granger, and Bernardo L. Sabatini. 2016. 'Mechanisms and Functions of GABA Co-Release'. *Nature Reviews Neuroscience* 17 (3): 139–45. https://doi.org/10.1038/nrn.2015.21.

Tritsch, Nicolas X, Won-Jong Oh, Chenghua Gu, and Bernardo L Sabatini. 2014. 'Midbrain Dopamine Neurons Sustain Inhibitory Transmission Using Plasma Membrane Uptake of GABA, Not Synthesis'. *eLife* 3 (April):e01936. https://doi.org/10.7554/eLife.01936.

Trudeau, Louis-Eric, Thomas S. Hnasko, Åsa Wallén-Mackenzie, Marisela Morales, Steven Rayport, and David Sulzer. 2014. 'The Multilingual Nature of Dopamine Neurons'. In *Progress in Brain Research*, 211:141–64. Elsevier. https://doi.org/10.1016/B978-0-444-63425-2.00006-4.

Wang, Yuwei, Pei Zhang, Yulin Chao, Zhini Zhu, Chuanhui Yang, Zixuan Zhou, Yaohui Li, et al. 2024. 'Transport and Inhibition Mechanism for VMAT2-Mediated Synaptic Vesicle Loading of Monoamines'. *Cell Research* 34 (1): 47–57. https://doi.org/10.1038/s41422-023-00906-z.

Watkins, Jeffrey C, and David E Jane. 2006. ‘The Glutamate Story’. *British Journal of Pharmacology* 147 (S1). https://doi.org/10.1038/sj.bjp.0706444.

Zhang, Wen, Bing-Rui Xiong, Long-Qing Zhang, Xian Huang, Xiaoman Yuan, Yu-Ke Tian, and Xue-Bi Tian. 2021. ‘The Role of the GABAergic System in Diseases of the Central Nervous System’. *Neuroscience* 470 (August):88–99. https://doi.org/10.1016/j.neuroscience.2021.06.037.

Zhu, Angqi, Junhao Huang, Fang Kong, Jiaxin Tan, Jianlin Lei, Yafei Yuan, and Chuangye Yan. 2023. ‘Molecular Basis for Substrate Recognition and Transport of Human GABA Transporter GAT1’. *Nature Structural & Molecular Biology* 30 (7): 1012–22. https://doi.org/10.1038/s41594-023-00983-z.

7 Tables

8 Figures